

Sparse Activity Detection for Massive Connectivity

Zhilin Chen, *Student Member, IEEE*, Foad Sahrabi, *Student Member, IEEE*, and Wei Yu, *Fellow, IEEE*

Abstract—This paper considers the massive connectivity application in which a large number of potential devices communicate with a base-station (BS) in a sporadic fashion. The detection of device activity pattern together with the estimation of the channel are central problems in such a scenario. Due to the large number of potential devices in the network, the devices need to be assigned non-orthogonal signature sequences. The main objective of this paper is to show that by using random signature sequences and by exploiting sparsity in the user activity pattern, the joint user detection and channel estimation problem can be formulated as a compressed sensing single measurement vector (SMV) problem or multiple measurement vector (MMV) problem, depending on whether the BS has a single antenna or multiple antennas, and be efficiently solved using an approximate message passing (AMP) algorithm. This paper proposes an AMP algorithm design that exploits the statistics of the wireless channel and provides an analytical characterization of the probabilities of false alarm and missed detection by using the state evolution. We consider two cases depending on whether the large-scale component of the channel fading is known at the BS and design the minimum mean squared error (MMSE) denoiser for AMP according to the channel statistics. Simulation results demonstrate the substantial advantage of exploiting the statistical channel information in AMP design; however, knowing the large-scale fading component does not offer tangible benefits. For the multiple-antenna case, we employ two different AMP algorithms, namely the AMP with vector denoiser and the parallel AMP-MMV, and quantify the benefit of deploying multiple antennas at the BS.

Index Terms—Device activity detection, channel estimation, approximate message passing, compressed sensing, Internet of Things (IoT), machine-type communications (MTC)

I. INTRODUCTION

One of the key requirements for the next-generation wireless cellular networks is to provide massive connectivity for machine-type communications (MTC), envisioned to support diverse applications such as environment sensing, event detection, surveillance and control [1], [2]. Machine-centric communications have two distinctive features as compared to conventional human-centric communications: (i) the overall system needs to support massive connectivity—the number of devices connected to each cellular base-station (BS) may be in the order of 10^4 to 10^6 ; and (ii) the traffic pattern of each device may be sporadic—at any given time only a small fraction of potential devices are active. For such a network, accurate user activity detection and channel estimation are

crucial for establishing successful communications between the devices and the BS.

To identify active users and to estimate their channels, each user must be assigned a unique signature sequence. However, due to the large number of potential devices but the limited coherence time and frequency dimensions in the wireless fading channel, the signature sequences for all users cannot be mutually orthogonal. Non-orthogonal signature sequences superimposed in the pilot stage causes significant multi-user interference, e.g., when a simple matched filtering or correlation operation is applied at the BS for user activity detection and channel estimation. A key observation of this paper is that the sporadic nature of the traffic leads to *sparse* user transmission patterns. By exploiting sparsity and by formulating the detection and estimation problem with independent identically distributed (i.i.d.) random non-orthogonal pilots as a compressed sensing problem, this multi-user interference problem can be overcome, and highly reliable activity detection and accurate channel estimation can be made possible. In the compressed sensing terminology, when the BS is equipped with a single antenna, activity detection and channel estimation can be formulated as a single measurement vector (SMV) problem; when the BS has multiple antennas, the problem can be formulated as a multiple measurement vector (MMV) problem.

This paper proposes the use of compressed sensing techniques for the joint user activity detection and channel estimation problem. Due to the large-scale nature of massive device communications, this paper adopts the computationally efficient approximate message passing (AMP) algorithm [3] as the main technique. AMP is an iterative thresholding method with a key feature that allows analytic performance characterization via the so-called state evolution. The main contributions of this paper are: (i) a novel AMP algorithm design for user activity detection that exploits the statistical information of the wireless channel; and (ii) a characterization of the probabilities of false alarm and missed detection for both SMV and MMV scenarios.

A. Related Work

The user activity detection problem for massive connectivity has been studied from information theoretical perspectives in [2], [4]. From an algorithmic point of view, the problem is closely related to sparse recovery in compressed sensing and has been studied in a variety of wireless communication settings. For example, assuming no prior knowledge of the channel state information (CSI), joint user activity detection and channel estimation is considered in [5]–[8]. Specifically, [5] proposes an efficient greedy algorithm based on orthogonal matching pursuit for sporadic multi-user communication. By

Manuscript accepted and to appear in IEEE Transactions on Signal Processing. This work has been presented in part at IEEE International Conference on Acoustics, Speech, and Signal Processing (ICASSP), March 2017. This work is supported by Natural Sciences and Engineering Research Council (NSERC) of Canada through a Discovery Grant and through a Steacie Memorial Fellowship.

The authors are with The Edward S. Rogers Sr. Department of Electrical and Computer Engineering, University of Toronto, Toronto, ON M5S 3G4, Canada (e-mails: {zchen, fsahrabi, weiyu}@comm.utoronto.ca).

exploiting the statistics of channel path-loss and the joint sparsity structures, [6] proposes a modified Bayesian compressed sensing algorithm in a cloud radio-access network. In the context of orthogonal frequency division multiplexing (OFDM) systems, [7] introduces a one-shot random access protocol and employs the basis pursuit denoising detection method with a detection error bound based on the restricted isometry property. The performance of such schemes in a practical setting is illustrated in [7], [8]. When perfect CSI is assumed, joint user activity and data detection for code division multiple access systems (CDMA) is investigated in [9], [10], where [9] designs the sparsity-exploiting maximum a posteriori detector by accounting for both sparsity and finite-alphabet constraints of the signal, and [10] proposes a greedy block-wise orthogonal least square algorithm by exploiting the block sparsity among several symbol durations. Differing from most of the above works that consider cellular systems, [11], [12] study the user activity detection in wireless ad hoc networks, where each node in the system identifies its neighbor nodes simultaneously. The authors of [11] propose a scalable compressed neighbor discovery scheme that employs random binary signatures and group testing based detection algorithms. In [12], the authors propose a more dedicated scheme that uses signatures based on Reed-Muller code and a chirp decoding algorithm to achieve a better performance.

In contrast to the aforementioned works, this paper adopts the more computationally efficient AMP algorithm for user activity detection and channel estimation, which is more suitable for large-scale networks with a large number of devices. The AMP algorithm is first proposed in [3] as a low-complexity iterative algorithm for conventional compressed sensing with real-valued signals and real-valued measurements. A framework of state evolution that tracks the performance of AMP at each iteration is introduced in [3]. The AMP algorithm is then extended along different directions. For example, [13] generalizes the AMP algorithm to a broad family of iterative thresholding algorithms, and provides a rigorous proof of the framework of the state evolution. To deal with complex-valued signals and measurements, [14] proposes a complex AMP algorithm (CAMP). By exploiting the input and output distributions, a generalized AMP (GAMP) algorithm is designed in [15]. Similarly, a Bayesian approach is used to design the AMP algorithm in [16], [17] by accounting for the input distribution. For the compressed sensing problem with multiple signals sharing joint sparsity, i.e., the MMV problem, [18] designs an AMP algorithm via a vector form of message passing; and [19] designs the AMP-MMV algorithm by directly using message passing over a multi-frame factor graph.

Although the use of the AMP algorithm for user activity detection has been previously proposed in [20], the statistical information of the channel is not exploited in the prior work; also performance analysis is not yet available. This paper makes progress by showing that exploiting channel statistics can significantly enhance the Bayesian AMP algorithm. Moreover, analytical performance characterization can be obtained by using state evolution. Finally, the AMP algorithm can be extended to the multiple-antenna case.

B. Main Contributions

This paper considers the user activity detection and channel estimation problem in the uplink of a single-cell network with a large number of potential users, but at any given time slot only a small fraction of them are active. To exploit the sparsity in user activity pattern, this paper formulates the problem as a compressed sensing problem and proposes the use of random signature sequences and the computationally efficient AMP algorithm for device activity detection. This paper provides the design and analysis of AMP for both cases in which the BS is equipped with a single antenna and with multiple antennas.

This paper considers two different scenarios: (i) when the large-scale fading coefficients of all user are known and the detector is designed based on the statistics of fast fading component only; and (ii) when the large-scale fading coefficients are not known and the detector is designed based on the statistics of both fast fading and large-scale fading components as a function of the distribution of device locations in the cell. The proposed AMP-based detector exploits the statistics of the wireless channel by specifically designing the minimum mean squared error (MMSE) denoiser. This paper provides analytical characterization of the probabilities of false alarm and missed detection via the state evolution for both scenarios.

For the case where the BS is equipped with a single antenna, numerical results indicate that: (i) the analytic performance characterization via state evolution is very close to the simulation; (ii) exploiting the statistical information of the channel and user activity can significantly improve the detector performance; and (iii) knowing the large-scale fading coefficient actually does not bring substantial performance improvement as compared to the case that only the statistical information about the large-scale fading is available.

For the case where the BS is equipped with multiple antennas, this paper considers both the AMP with vector denoiser [18] and the parallel AMP-MMV [17]. For the AMP with vector denoiser, this paper exploits wireless channel statistics in denoiser design and further analytically characterizes the probabilities of false alarm and missed detection based on the state evolution. For the parallel AMP-MMV algorithm, which is more suitable for distributed computation, performance characterization is more difficult to obtain. Simulation results show that: (i) having multiple antennas at the BS can significantly improve the detector performance; (ii) the predicted performance of AMP with vector denoiser is very close to its simulated performance; and (iii) AMP with vector denoiser and parallel AMP-MMV achieve approximately the same performance.

C. Paper Organization and Notations

The remainder of this paper is organized as follows. Section II introduces the system model. Section III introduces the AMP algorithms for both SMV and MMV problems. Section IV considers user activity detection and channel estimation when the BS has a single-antenna, while Section V considers the multiple-antenna case. Simulation results are provided in Section VI. Conclusions are drawn in Section VII.

Throughout this paper, upper-case and lower-case letters denote random variables and their realizations, respectively. Boldface lower-case letters denote vectors. Boldface upper-case letters denote matrices or random vectors, where context should make the distinction clear. Superscripts $(\cdot)^T$, $(\cdot)^*$ and $(\cdot)^{-1}$ denote transpose, conjugate transpose, and inverse operators, respectively. Further, \mathbf{I} denotes identity matrix with appropriate dimensions, $\mathbb{E}[\cdot]$ denotes expectation operation, \triangleq denotes definition, $|\cdot|$ denotes either the magnitude of a complex variable or the determinant of a matrix, depending on the context, and $\|\cdot\|_2$ denotes the ℓ_2 norm.

II. SYSTEM MODEL

Consider the uplink of a wireless cellular system with one BS located at the center and N single-antenna devices located uniformly in a circular area with radius R , but in each coherence block only a subset of users are active. Let $a_n \in \{1, 0\}$ indicate whether or not user n is active. For the purpose of channel probing and user identification, user n is assigned a unique signature sequence $\mathbf{s}_n = [s_{1n}, s_{2n}, \dots, s_{Ln}]^T \in \mathbb{C}^{L \times 1}$, where L is the length of the sequence. This paper assumes that the signature sequence \mathbf{s}_n is generated according to i.i.d. complex Gaussian distribution with zero mean and variance $1/L$ such that each sequence is normalized to have unit power, and the normalization factor $1/L$ is incorporated into the transmit power.

We consider a block-fading channel model where the channel is static in each block. In this paper, we consider two cases where the BS is equipped with either a single antenna or multiple antennas. When the BS has only one antenna, the received signal at the BS can be modeled as

$$\mathbf{y} = \sum_{n=1}^N a_n \mathbf{s}_n h_n + \mathbf{w} \triangleq \mathbf{S}\mathbf{x} + \mathbf{w}, \quad (1)$$

where $h_n \in \mathbb{C}$ is the channel coefficient between user n and the BS, $\mathbf{w} \in \mathbb{C}^{L \times 1}$ is the effective complex Gaussian noise whose variance σ_w^2 depends on the background noise power normalized by the user transmit power. Here, $\mathbf{x} \triangleq [x_1, x_2, \dots, x_N]^T \in \mathbb{C}^{N \times 1}$ where $x_n \triangleq h_n a_n$, and $\mathbf{S} \triangleq [\mathbf{s}_1, \mathbf{s}_2, \dots, \mathbf{s}_N] \in \mathbb{C}^{L \times N}$.

We aim to recover the non-zero entries of \mathbf{x} based on the received signals \mathbf{y} . We are interested in the regime where the number of potential users is much larger than the pilot sequence length, i.e., $N \gg L$, so that the user pilot sequences cannot be mutually orthogonal; but due to the sporadic traffic, only a small number of devices transmit in each block, resulting in a sparse \mathbf{x} . The recovering of \mathbf{x} for the single antenna case is in the form of the SMV problem in compressed sensing.

This paper also considers the case where the BS is equipped with M antennas. In this case, the received signal $\mathbf{Y} \in \mathbb{C}^{L \times M}$ at the BS can be expressed in matrix form as

$$\mathbf{Y} = \sum_{n=1}^N a_n \mathbf{s}_n \mathbf{h}_n + \mathbf{W} \triangleq \mathbf{S}\mathbf{X} + \mathbf{W}, \quad (2)$$

where $\mathbf{h}_n \in \mathbb{C}^{1 \times M}$ is the channel vector between user n and the BS, $\mathbf{W} \in \mathbb{C}^{L \times M}$ is the effective complex Gaussian noise,

and $\mathbf{X} \triangleq [\mathbf{r}_1^T, \dots, \mathbf{r}_N^T]^T \in \mathbb{C}^{N \times M}$ where $\mathbf{r}_n \triangleq a_n \mathbf{h}_n \in \mathbb{C}^{1 \times M}$ is the n th row vector of \mathbf{X} . We also use $\mathbf{c}_m \in \mathbb{C}^{N \times 1}$ to represent the m th column vector of \mathbf{X} , i.e., $\mathbf{X} = [\mathbf{c}_1, \dots, \mathbf{c}_M]$. Note that a_n indicates whether the entire row vector \mathbf{r}_n is zero or not. In other words, columns of \mathbf{X} (i.e., \mathbf{c}_m) share the same sparsity pattern.

We are interested in detecting the user activity a_n as well as in estimating the channel gains of the active users, which correspond to the non-zero rows of the matrix \mathbf{X} , based on the observation \mathbf{Y} in the regime where $N \gg L$. The problem of recovering \mathbf{X} from \mathbf{Y} is in the form of the MMV problem in compressed sensing.

A key observation of this paper is that the design of recovery algorithm can be significantly enhanced by taking advantage of the knowledge about the statistical information of \mathbf{x} or \mathbf{X} . Toward this end, we provide a model for the distribution of the entries of \mathbf{x} , and the distribution of the rows of \mathbf{X} . Since \mathbf{x} is a special case of \mathbf{X} when $M = 1$, we focus on the model for \mathbf{X} .

We assume that each user accesses the channel with a small probability λ in an i.i.d. fashion, i.e., $\Pr(a_n = 1) = \lambda, \forall n$, and there is no correlation between different users' channels, so that the row vectors of \mathbf{X} follow a mixture distribution

$$p_{\mathbf{R}|G}(\mathbf{r}_n | g_n) = (1 - \lambda)\delta_0 + \lambda p_{\mathbf{H}|G}(\mathbf{r}_n | g_n), \quad (3)$$

where δ_0 denotes the point mass measure at $\mathbf{0}$, $p_{\mathbf{H}|G}$ denotes the probability density function (pdf) of the channel vector \mathbf{H} given prior information G , which has a pdf p_G , and g_n denotes the prior information for user n . Note that we use \mathbf{H} to denote the random channel vector and \mathbf{h}_n to denote its realization. Based on (3), the pdf of the entries of \mathbf{x} is

$$p_{X|G}(x_n | g_n) = (1 - \lambda)\delta_0 + \lambda p_{H|G}(x_n | g_n). \quad (4)$$

To model the distribution of \mathbf{H} , we assume that all users are randomly and uniformly located in a circular coverage area of radius R with the BS at the center, and the channels between the users and the BS follow an independent distribution that depends on the distance. More specifically, \mathbf{H} includes path-loss, shadowing, and Rayleigh fading. The path-loss between a user and the BS is modeled (in dB) as $\alpha + \beta \log_{10}(d)$, where d is the distance measured in meter, α is the fading coefficient at $d = 1$, and β is the path-loss exponent. The shadowing (in dB) follows a Gaussian distribution with zero mean and variance σ_{SF}^2 . The Rayleigh fading is assumed to be i.i.d. complex Gaussian with zero mean and unit variance across all antennas.

The large-scale fading, which includes path-loss and shadowing, is denoted as G , whose pdf p_G can be modeled by the distribution of BS-user distance and shadowing parameter σ_{SF}^2 . This paper considers both the case where only the statistics of the the large-scale fading, i.e., p_G , is known as well as the case where the exact large-scale fading coefficient g_n is known at the BS. The latter case is motivated by the scenario in which the devices are stationary, so that the path-loss and shadowing can be estimated and stored at the BS as prior information. When g_n is known, $p_{\mathbf{H}|G}$ captures the distribution of the Rayleigh fading component. When only $p(G)$ is known, we drop G and g_n from $p_{\mathbf{H}|G}(\mathbf{h}_n | g_n)$, and write it as $p_{\mathbf{H}}(\mathbf{h}_n)$,

which captures the distribution of both large-scale fading and Rayleigh fading.

III. AMP ALGORITHM

AMP is an iterative algorithm that recovers sparse signal for compressed sensing. We introduce the AMP framework for both the SMV and the MMV problems in this section.

A. AMP for SMV problem

AMP is first proposed for the SMV problem in [3]. Starting with $\mathbf{x}^0 = \mathbf{0}$ and $\mathbf{z}^0 = \mathbf{y}$, AMP proceeds at each iteration as

$$\mathbf{x}^{t+1} = \eta(\mathbf{S}^* \mathbf{z}^t + \mathbf{x}^t, \mathbf{g}, t), \quad (5)$$

$$\mathbf{z}^{t+1} = \mathbf{y} - \mathbf{S} \mathbf{x}^{t+1} + \frac{N}{L} \mathbf{z}^t \langle \eta'(\mathbf{S}^* \mathbf{z}^t + \mathbf{x}^t, \mathbf{g}, t) \rangle, \quad (6)$$

where $\mathbf{g} \triangleq [g_1, \dots, g_N]^T$, and $t = 0, 1, \dots$ is the index of iteration, \mathbf{x}^t is the estimate of \mathbf{x} at iteration t , \mathbf{z}^t is the residual, $\eta(\cdot, \mathbf{g}, t) \triangleq [\eta_t(\cdot, g_1), \dots, \eta_t(\cdot, g_N)]^T$ where $\eta_t(\cdot, g_n) : \mathbb{C} \rightarrow \mathbb{C}$ is an appropriately designed non-linear function known as *denoiser* that operates on the n th entry of the input vector, $\eta'(\cdot) \triangleq [\eta'_t(\cdot, g_1), \dots, \eta'_t(\cdot, g_N)]^T$ where $\eta'_t(\cdot, g_n)$ is the first order derivative of $\eta_t(\cdot, g_n)$ with respect to the first argument, and $\langle \cdot \rangle$ is averaging operation over all entries of a vector. Note that the third term in the right hand side of (6) is the correction term known as the ‘‘Onsager term’’ from statistical physics.

In the AMP algorithm, the matched filtered output $\tilde{\mathbf{x}}^t \triangleq \mathbf{S}^* \mathbf{z}^t + \mathbf{x}^t$ can be modeled as signal \mathbf{x} plus noise (including multiuser interference), i.e., $\tilde{\mathbf{x}}^t = \mathbf{x} + \mathbf{v}^t$, where \mathbf{v}^t is Gaussian due to the correction term. The denoiser is typically designed to reduce the estimation error at each iteration. In the compressed sensing literature, the prior distribution of \mathbf{x} is usually assumed to be unknown. In this case, a minimax framework over the worst case \mathbf{x} leads to a soft thresholding denoiser [21]. When the prior distribution of \mathbf{x} is known, the Bayesian framework then can be used to account for the prior information on \mathbf{x} [16]. In this paper, we adopt the Bayesian approach and design the MMSE denoiser for the massive connectivity setup as shown in the next section.

The AMP algorithm can be analyzed in the asymptotic regime where $L, N \rightarrow \infty$ with fixed N/L via the state evolution, which predicts the per-coordinate performance of the AMP algorithm at each iteration as follows

$$\tau_{t+1}^2 = \sigma_w^2 + \frac{N}{L} \mathbb{E}[|\eta_t(X + \tau_t V, G) - X|^2], \quad (7)$$

where τ_t is referred to as the *state*, X , V , and G are random variables with X following $p_{X|G}$, V following the complex Gaussian distribution with zero mean and unit variance, and G following p_G , and the expectation is taken over all X , V , and G . We denote $\tilde{X}^t \triangleq X + \tau_t V$. The random variables X , V , G , \tilde{X}^t capture the distributions of the entries of \mathbf{x} , entries of \mathbf{v}^t (up to a factor τ_t), the prior information g_n , and entries of $\tilde{\mathbf{x}}^t$, respectively, with $\mathbb{E}[|\eta_t(\tilde{X}^t, G) - X|^2]$ characterizing the per-coordinate MSE of the estimate of \mathbf{x} at iteration t .

B. AMP for MMV problem

1) *AMP with vector denoiser*: One extension of the AMP algorithm to solve the MMV problem in (2) is proposed in [18], which employs a vector denoiser that operates on each row vector of the matched filtered output:

$$\mathbf{X}^{t+1} = \eta(\mathbf{S}^* \mathbf{Z}^t + \mathbf{X}^t, \mathbf{g}, t), \quad (8)$$

$$\mathbf{Z}^{t+1} = \mathbf{Y} - \mathbf{S} \mathbf{X}^{t+1} + \frac{N}{L} \mathbf{Z}^t \langle \eta'(\mathbf{S}^* \mathbf{Z}^t + \mathbf{X}^t, \mathbf{g}, t) \rangle, \quad (9)$$

where $\eta(\cdot, \mathbf{g}, t) \triangleq [\eta_t(\cdot, g_1), \dots, \eta_t(\cdot, g_N)]^T$ with $\eta_t(\cdot, g_n) : \mathbb{C}^{1 \times M} \rightarrow \mathbb{C}^{1 \times M}$ is a vector denoiser that operates on the n th row vector of $\mathbf{S}^* \mathbf{Z}^t + \mathbf{X}^t$, and the other notations are similar to those used in (5) and (6). The state evolution of the AMP algorithm for the MMV problem also has a similar form as

$$\Sigma_{t+1} = \sigma_w^2 \mathbf{I} + \frac{N}{L} \mathbb{E}[\mathbf{D}^t (\mathbf{D}^t)^*], \quad (10)$$

where $\mathbf{D}^t \triangleq (\eta_t(\mathbf{R} + \mathbf{U}^t, G) - \mathbf{R})^T \in \mathbb{C}^{M \times 1}$, with random vector \mathbf{R} following $p_{\mathbf{R}|G}$ and random vector \mathbf{U}^t following $\mathcal{CN}(\mathbf{0}, \Sigma_t)$. The expectation is taken over \mathbf{R} , \mathbf{U}^t , and G . To minimize the estimation error at each iteration, we can also design the vector denoiser $\eta_t(\cdot, \cdot)$ via the Bayesian approach.

2) *Parallel AMP-MMV*: A different extension of the AMP algorithm for dealing with the MMV problem is the parallel AMP-MMV algorithm proposed in [19]. The basic idea is to solve the MMV problem iteratively by using multiple parallel AMP-SMVs then exchanging soft information between them. Parallelization allows distributed implementation of the algorithm, which can be computationally advantageous, especially when the number of antennas is large.

The outline of the parallel AMP-MMV algorithm is illustrated in Algorithm 1 which operates on a per-antenna basis, i.e., on the columns of \mathbf{X} and \mathbf{Z} , denoted as \mathbf{c}_m and \mathbf{z}_m respectively, and where $\eta(\cdot, \mathbf{g}, t, i, m) \triangleq [\eta_{t,i,m}(\cdot, g_1), \dots, \eta_{t,i,m}(\cdot, g_N)]^T$ is the denoiser used for the m th antenna in the iteration (t, i) . Note that here we add index i and m in the notation of denoiser, $\eta_{t,i,m}(\cdot, g_n)$, to indicate the index of outer iteration and the index of SMV stage, respectively. In the first phase which is called the (into)-phase, the messages $\tilde{\pi}_{nm}$ are calculated and passed to the m th AMP-SMV stage. These messages convey the current belief about the probability of being active for each user. In the first iteration, we have $\tilde{\pi}_{nm} = \lambda, \forall n, m$, since no further information is available. In the next phase, which is called the (within)-phase, the conventional AMP algorithm is applied to the received signal of each antenna. Note that the denoiser in AMP algorithm is a function of the current belief about the activity of the users which is obtained based on the information sharing between all M AMP-SMV stages. Finally, in the (out)-phase, the estimate of channel gains is used to refine the belief about the activity of the users.

IV. USER ACTIVITY DETECTION: SINGLE-ANTENNA CASE

A main point of this paper is that exploiting the statistics of the wireless channel can significantly enhance detector performance. This section proposes an MMSE denoiser design for the AMP algorithm for the wireless massive connectivity

Algorithm 1 Parallel AMP-MMV Method [19]

-
- 1: Initialize $\vec{\pi}_{nm} = 0.5, \forall n, m$.
 - 2: **for** $i = 1$ to I **do**
Execute the (into)-phase:
 - 3: $\overleftarrow{\pi}_{nm} = \frac{\lambda \prod_{m' \neq m} \overleftarrow{\pi}_{nm'}}{(1-\lambda) \prod_{m' \neq m} (1-\overleftarrow{\pi}_{nm'}) + \lambda \prod_{m' \neq m} \overleftarrow{\pi}_{nm'}}, \forall n, m$
Execute the (within)-phase:
 - 4: **for** $m = 1$ to M **do**
 - 5: Initialize $\mathbf{c}_m^0 = \mathbf{0}, \mathbf{z}_m^0 = \mathbf{y}_m$.
 - 6: **for** $t = 0$ to T **do**
 - 7: $\mathbf{c}_m^{t+1} = \eta(\mathbf{S}^* \mathbf{z}_m^t + \mathbf{c}_m^t, \mathbf{g}, t, i, m)$,
 - 8: $\mathbf{z}_m^{t+1} = \mathbf{y}_m - \mathbf{S} \mathbf{c}_m^{t+1} + \frac{N}{L} \mathbf{z}_m^t \langle \eta'(\mathbf{S}^* \mathbf{z}_m^t + \mathbf{c}_m^t, \mathbf{g}, t, i, m) \rangle$,
 - 9: **end for**
 - 10: **end for**
Execute the (out)-phase:
 - 11: Calculate $\vec{\pi}_{nm}, \forall n, m$, the probability of user n being active based on the decision at the m th AMP-SMV stage.
 - 12: **end for**
-

problem that specifically takes wireless channel characteristics into consideration in the single-antenna case. Two scenarios are considered: the large-scale fading g_n of each user is either directly available or only its statistics is available at the BS. This section further studies the optimal detection strategy, and analyzes the probabilities of false alarm and missed detection by using the state evolution of the AMP algorithm.

A. MMSE Denoiser for AMP Algorithm

In the scenario where only the statistics about the large-scale fading is known at the BS, the distributions of the channel coefficients $p_H(h_n)$ are independent and identical for all devices. In the scenario where the devices are stationary and their path-loss and shadowing coefficients can be estimated and thus the exact large-scale fading is known at the BS, the distributions of the channel coefficients are of the form $p_{H|G}(h_n|g_n)$, which are complex Gaussian with variance parameterized by g_n , and are independent but not identical across the devices. To derive the MMSE denoisers via the Bayesian approach for both cases, we first characterize the distributions $p_G(g_n)$, $p_H(h_n)$ and $p_{H|G}(h_n|g_n)$ as follows.

Proposition 1. Consider a circular wireless cellular coverage area of radius R with BS at the center and uniformly distributed devices where the channels between the BS and the devices are modeled with large-scale fading g_n with parameters α, β and shadowing fading parameter σ_{SF} as defined in the system model. Then, g_n follows a distribution as

$$p_G(g_n) = a g_n^{-\gamma} Q(g_n), \quad (11)$$

where $Q(g_n) \triangleq \int_{(b \ln g_n + c)}^{\infty} \exp(-s^2) ds$, $\gamma \triangleq 40/\beta + 1$, and a, b , and c are constants depending on parameters $\alpha, \beta, \sigma_{\text{SF}}$ and R as

$$a = \frac{40}{R^2 \beta \sqrt{\pi}} \exp\left(\frac{2(\ln 10)^2 \sigma_{\text{SF}}^2}{\beta^2} - \frac{2 \ln(10) \alpha}{\beta}\right),$$

$$b = \frac{-10\sqrt{2}}{(\ln 10)\sigma_{\text{SF}}}, \quad c = \frac{-\alpha - \beta \log_{10}(R)}{\sqrt{2}\sigma_{\text{SF}}} - \frac{20}{\beta b}.$$

Proof. See Appendix A. \square

Proposition 2. Denote h_n as the channel coefficient which contains both the large-scale fading g_n and Rayleigh fading. If only $p_G(g_n)$ is known at the BS, the pdf of h_n is given by

$$p_H(h_n) = \int_0^\infty \frac{a}{\pi} g_n^{-\gamma-2} Q(g_n) \exp\left(\frac{-|h_n|^2}{g_n^2}\right) dg_n. \quad (12)$$

If g_n is known at the BS, the pdf of h_n given g_n is

$$p_{H|G}(h_n|g_n) = \frac{1}{\pi g_n^2} \exp\left(\frac{-|h_n|^2}{g_n^2}\right). \quad (13)$$

Proof. See Appendix B. \square

Note that for the first scenario, the channel distribution (12) only depends on a few parameters such as the path-loss exponent in the path-loss model and the standard deviation in the shadowing model, which are assumed to be known and can be estimated in practice. For the second scenario, the channel distribution (13) is just a Rayleigh fading model parameterized by the large-scale fading. The large-scale fading information can be obtained by tracking the estimated channel over a reasonable period. This second scenario is applicable to the case where the users are mostly stationary, so the large-scale fading changes only slowly over time. It is worth noting that although this paper restricts attention to the Rayleigh fading model, the approach developed here is equally applicable for Rician or any other statistical channel model.

In the following, we design the MMSE denoisers for the AMP algorithm by exploiting $p_H(h_n)$ and $p_{H|G}(h_n|g_n)$.

1) *With Statistical Knowledge of Large-Scale Fading Only:* Since g_n is unknown and only the distribution $p_G(g_n)$ is available at the BS, the denoiser $\eta_t(\cdot, g_n)$ reduces to $\eta_t(\cdot)$, which indicates that the denoiser for each entry of the matched filtered output is the same. By using (12), the pdf of the entries of \mathbf{x} can be expressed as

$$p_X(x_n) = (1 - \lambda)\delta_0 + \int_0^\infty \frac{\exp(-|x_n|^2 g_n^{-2})}{\pi g_n^{\gamma+2} / (a \lambda Q(g_n))} dg_n. \quad (14)$$

The MMSE denoiser is given by the conditional expectation, i.e., $\eta_t(\tilde{x}_n^t) = \mathbb{E}[X|\tilde{X}^t = \tilde{x}_n^t]$ where random variable $\tilde{X}^t = X + \tau_t V$, and \tilde{x}_n^t is a realization of \tilde{X}^t . Note that the denoiser $\eta_t(\tilde{x}_n^t)$ depends on t through τ_t . The expression of the conditional expectation is given in the following proposition.

Proposition 3. Based on the pdf of x_n in (14) and the signal-plus-noise model $\tilde{X}^t = X + \tau_t V$ at each iteration in AMP, the conditional expectation of X given $\tilde{X}^t = \tilde{x}_n^t$ is given by

$$\mathbb{E}[X|\tilde{X}^t = \tilde{x}_n^t] = \tilde{x}_n^t \frac{\nu_1(|\tilde{x}_n^t|^2)}{\xi_1(|\tilde{x}_n^t|^2)}, \quad (15)$$

where functions $\nu_i(s)$ and $\xi_i(s)$ are defined as

$$\nu_i(s) \triangleq \int_0^\infty \frac{g_n^{2-\gamma} Q(g_n)}{(g_n^2 + \tau_t^2)^{i+1}} \exp\left(\frac{-s}{g_n^2 + \tau_t^2}\right) dg_n, \quad (16)$$

$$\xi_i(s) \triangleq \frac{1 - \lambda}{\lambda a \tau_t^{2i}} \exp\left(\frac{-s}{\tau_t^2}\right) + \int_0^\infty \frac{g_n^{-\gamma} Q(g_n)}{(g_n^2 + \tau_t^2)^i} \exp\left(\frac{-s}{g_n^2 + \tau_t^2}\right) dg_n. \quad (17)$$

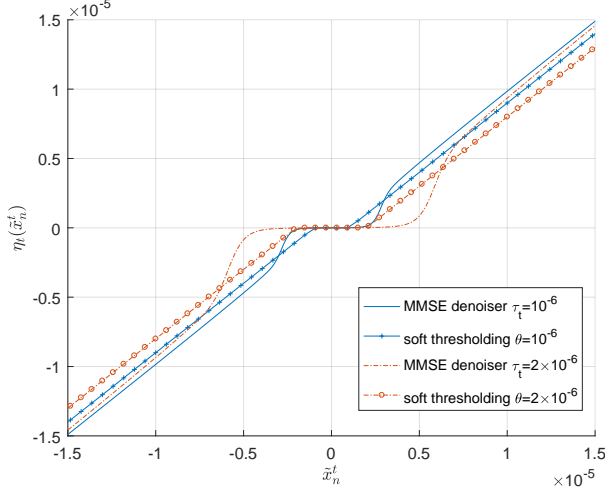


Fig. 1. MMSE denoiser vs. soft thresholding denoiser [14] $\eta_t^{\text{soft}}(\tilde{x}_n^t) \triangleq (\tilde{x}_n^t - \frac{\theta \tilde{x}_n^t}{|\tilde{x}_n^t|}) \mathbb{I}(|\tilde{x}_n^t| > \theta)$, where $\mathbb{I}(\cdot)$ is the indicator function.

Proof. See Appendix C. \square

Note that to implement $\eta_t(\tilde{x}_n^t)$ at each iteration, the value of τ_t is needed. In practice, an empirical estimate $\hat{\tau}_t = \frac{1}{\sqrt{L}} \|\mathbf{z}^t\|_2$, where $\|\cdot\|_2$ denotes the ℓ_2 norm, can be used [22]. Although $\eta_t(\tilde{x}_n^t)$ is in a complicated form, we note that it can be pre-computed and stored as table lookup, so it does not add to runtime complexity. To gain some intuition, we illustrate the shape of the MMSE denoiser as compared to the widely used soft thresholding denoiser in Fig. 1. We observe that the MMSE denoiser plays a role similar to the soft thresholding denoiser, shrinking the input towards the origin, especially when the input is small, thereby promoting sparsity.

2) *With Exact Knowledge of Large-Scale Fading:* When g_n is available at the BS, we substitute (13) into (4), and the pdf of the entries of \mathbf{x} is simplified to Bernoulli-Gaussian as

$$p_{X|G}(x_n|g_n) = (1 - \lambda)\delta_0 + \frac{\lambda}{\pi g_n^2} \exp\left(\frac{-|x_n|^2}{g_n^2}\right). \quad (18)$$

The MMSE denoiser is given by $\eta_t(\tilde{x}_n^t, g_n) = \mathbb{E}[X|\tilde{X}^t = \tilde{x}_n^t, G = g_n]$, where the conditional expectation is [17]

$$\mathbb{E}[X|\tilde{X}^t = \tilde{x}_n^t, G = g_n] = \frac{g_n^2(g_n^2 + \tau_t^2)^{-1}\tilde{x}_n^t}{1 + \frac{1-\lambda}{\lambda} \frac{g_n^2 + \tau_t^2}{\tau_t^2} \exp(-\Delta|\tilde{x}_n^t|^2)}, \quad (19)$$

where

$$\Delta \triangleq \tau_t^{-2} - (g_n^2 + \tau_t^2)^{-1}. \quad (20)$$

Compared with the MMSE denoiser in (15), we add g_n to the left hand side of (19) to emphasize the dependency on prior information g_n .

B. User Activity Detection

After the AMP algorithm has converged, we employ the likelihood ratio test to perform user activity detection. For the

hypothesis testing problem

$$\begin{cases} H_0 : X = 0, \text{ inactive user,} \\ H_1 : X \neq 0, \text{ active user;} \end{cases} \quad (21)$$

the optimal decision rule is given by

$$\text{LLR} = \log \left(\frac{p_{\tilde{X}^t|X}(\tilde{x}_n^t|X \neq 0)}{p_{\tilde{X}^t|X}(\tilde{x}_n^t|X = 0)} \right) \underset{H_1}{\overset{H_0}{\gtrless}} l_n, \quad (22)$$

where LLR denotes the log-likelihood ratio, and l_n denotes the decision threshold typically determined by a cost function. The performance metrics of interest are the probability of missed detection P_M , defined as the probability that a device is active but the detector declare the null hypothesis H_0 , and the probability of false alarm, P_F , defined as the probability that a device is inactive, but the detector declare it to be active. We consider the threshold for two cases depending on whether the large-scale fading coefficient g_n is available at the BS or not.

1) *With Statistical Knowledge of Large-Scale Fading Only:* We first derive the likelihood probabilities in the following.

Proposition 4. Suppose that X follows (14), and V follows complex Gaussian distribution with zero mean and unit variance, the likelihood of $\tilde{X}^t = X + \tau_t V$ given $X = 0$ or $X \neq 0$ is given by

$$\begin{aligned} p_{\tilde{X}^t|X}(\tilde{x}_n^t|X = 0) &= \frac{1}{\pi \tau_t^2} \exp\left(\frac{-|\tilde{x}_n^t|^2}{\tau_t^2}\right), \\ p_{\tilde{X}^t|X}(\tilde{x}_n^t|X \neq 0) &= \int_0^\infty \frac{a g_n^{-\gamma} Q(g_n)}{\pi(g_n^2 + \tau_t^2)} \exp\left(\frac{-|\tilde{x}_n^t|^2}{g_n^2 + \tau_t^2}\right) dg_n. \end{aligned} \quad (23)$$

$$(24)$$

Proof. See Appendix D. \square

Based on (23) and (24), the log-likelihood ratio is given as

$$\text{LLR} = \log \int_0^\infty \frac{a \tau_t^2 g_n^{-\gamma}}{g_n^2 + \tau_t^2} Q(g_n) \exp(|\tilde{x}_n^t|^2 \Delta) dg_n, \quad (25)$$

where Δ is defined in (20). By observing that LLR is monotonic in $|\tilde{x}_n^t|$, we can simplify the decision rule in (22) as $|\tilde{x}_n^t| \underset{H_1}{\overset{H_0}{\gtrless}} l_n$, indicating that user activity detection can be performed based on the magnitude of \tilde{x}_n^t only.

Based on the likelihood probabilities and the threshold l_n , the probabilities of false alarm and missed detection can be characterized as follows

$$\begin{aligned} P_F &= \int_{|\tilde{x}_n^t| > l_n} p_{\tilde{X}^t|X}(\tilde{x}_n^t|X = 0) d\tilde{x}_n^t = \exp\left(\frac{-l_n^2}{\tau_t^2}\right), \\ P_M &= \int_{|\tilde{x}_n^t| < l_n} p_{\tilde{X}^t|X}(\tilde{x}_n^t|X \neq 0) d\tilde{x}_n^t, \end{aligned} \quad (26)$$

$$(27)$$

where (26) is simplified by using (23). Note that since only statistical information of the large-scale fading is known at the BS, P_F and P_M are the averaged false alarm and missed detection probabilities which do not depend on g_n .

2) *With Exact Knowledge of Large-Scale Fading:* When g_n is known at the BS, the distribution of X is simplified to Bernoulli-Gaussian. The likelihood probabilities become

$$p_{\tilde{X}^t|X,G}(\tilde{x}_n^t|X=0, G=g_n) = \frac{\exp(-|\tilde{x}_n^t|^2\tau_t^{-2})}{\pi\tau_t^2}, \quad (28)$$

$$p_{\tilde{X}^t|X,G}(\tilde{x}_n^t|X \neq 0, G=g_n) = \frac{\exp(-|\tilde{x}_n^t|^2(g_n^2 + \tau_t^2)^{-1})}{\pi(\tau_t^2 + g_n^2)}. \quad (29)$$

The log-likelihood ratio is then given as

$$\text{LLR}(g_n) = \log \left(\frac{\tau_t^2}{g_n^2 + \tau_t^2} \exp(|\tilde{x}_n^t|^2 \Delta) \right), \quad (30)$$

where the notation $\text{LLR}(g_n)$ emphasizes the dependency on the prior information g_n . Similar to the case where only the statistics of g_n is known, LLR here is also monotonic in $|\tilde{x}_n^t|$, which means that the user activity detection can be performed based on $|\tilde{x}_n^t|$ only.

We also use l_n to denote the threshold in the detection. Based on (28) and (29), the probabilities of false alarm and missed detection probability are given as follows

$$P_F(g_n) = \int_{|\tilde{x}_n^t| > l_n} p_{\tilde{X}^t|X,G}(\tilde{x}_n^t|X=0, G=g_n) d\tilde{x}_n^t \\ = \exp(-l_n^2\tau_t^{-2}), \quad (31)$$

$$P_M(g_n) = \int_{|\tilde{x}_n^t| < l_n} p_{\tilde{X}^t|X,G}(\tilde{x}_n^t|X \neq 0, G=g_n) d\tilde{x}_n^t \\ = 1 - \exp(-l_n^2(g_n^2 + \tau_t^2)^{-1}), \quad (32)$$

where we use the notation $P_F(g_n)$ and $P_M(g_n)$ to indicate the prior known g_n . Note that the false alarm probability in (31) has the form as that in (26) even through the value of τ_t may be different due to different denoisers.

A natural question then arises: how to design the threshold l_n as a function of the known large-scale fading g_n ? In theory, we can treat each user separately, i.e., set the thresholding value of each user separately according to its own cost function. For example, if a specific target false alarm probability is needed for user n , we can design its thresholding parameter, l_n , using the expression in (31). In order to bring fairness, this paper considers a common target false alarm probability for all users. Under this condition, all users share the same thresholding parameter, i.e., $l_n = l, \forall n$, since the expression of $P_F(g_n)$ in (31) does not depend on g_n . In such a case, different users may have different probabilities of missed detection depending on their large-scale fading g_n . To measure the performance of the detector for the entire system, we employ the average probability of missed detection as

$$\overline{P_M} = \frac{1}{N} \sum_{n=1}^N \left(1 - \exp\left(\frac{-l^2}{\tau_t^2 + g_n^2}\right) \right) \\ \rightarrow \int p_G(g) \left(1 - \exp\left(\frac{-l^2}{\tau_t^2 + g^2}\right) \right) dg, \text{ as } N \rightarrow \infty, \quad (33)$$

where the distribution $P_G(g)$ is given in (11). When N is large, once τ_t is given, the averaged performance only depends on the statistics of the large-scale fading g_n .

C. State Evolution Analysis

We have characterized the probabilities of false alarm P_F and missed detection P_M for user activity detection in (26), (27) and (31), (32), but the parameter τ_t that represents the standard deviation of the residual noise still needs to be determined. As AMP proceeds, τ_t converges to τ_∞ . To compute τ_t , we use the state evolution (7), where $\mathbb{E}[|\eta_t(\tilde{X}^t, G) - X|^2]$ in (7) can be interpreted as the MSE of the denoiser. Note that for the MMSE denoiser, MSE can also be expressed as $\mathbb{E}[|\eta_t(\tilde{X}^t, G) - X|^2] = \mathbb{E}[\text{Var}(X|\tilde{X}^t, G)]$, where $\text{Var}(X|\tilde{X}^t, G)$ is the conditional variance of X given \tilde{X}^t and G , and the expectation is taken over both \tilde{X}^t and G . (Note that we drop G if the large-scale fading coefficient is unknown.) By using conditional variance, we characterize the MSE of the designed denoisers in the following propositions.

Proposition 5. *The MSE of the denoiser for the case where only the statistics of g_n is known to the BS is given by*

$$\text{MSE}(\tau_t) = \int_0^\infty \frac{aQ(g_n)}{g_n^\gamma} \cdot \frac{\lambda g_n^2 \tau_t^2}{g_n^2 + \tau_t^2} dg_n \\ + \int_0^\infty a\lambda s (\mu_1(s) - \nu_1^2(s)\xi_1^{-1}(s)) ds, \quad (34)$$

where functions $\nu_i(s)$ and $\xi_i(s)$ are defined in (16) and (17), respectively, and function $\mu_i(s)$ is defined as

$$\mu_i(s) \triangleq \int_0^\infty \frac{g_n^{4-\gamma} Q(g_n)}{(g_n^2 + \tau_t^2)^{i+2}} \exp\left(\frac{-s}{g_n^2 + \tau_t^2}\right) dg_n. \quad (35)$$

Proof. See Appendix E. \square

It is worth noting that $\lambda g_n^2 \tau_t^2 (g_n^2 + \tau_t^2)^{-1}$ in the first term of the right hand side of (34) corresponds to the MSE of the estimate of x_n if the large-scale fading coefficient g_n as well as the user activity is assumed to be a priori known, and the integral of g_n corresponds to the averaging over all possible g_n . The second term then represents the cost of unknown g_n and unknown user activity in reality. Similarly, for the case where g_n is exactly known, the MSE can be characterized as follows.

Proposition 6. *The MSE of the denoiser for the case where g_n is known exactly at the BS is*

$$\text{MSE}(\tau_t) = \int_0^\infty \frac{aQ(g_n)}{g_n^\gamma} \cdot \frac{\lambda g_n^2 \tau_t^2}{g_n^2 + \tau_t^2} dg_n \\ + \int_0^\infty \frac{a\lambda Q(g_n) g_n^4}{g_n^\gamma (g_n^2 + \tau_t^2)} (1 - \varphi_1(g_n^2 \tau_t^{-2})) dg_n, \quad (36)$$

where function $\varphi_i(s)$ of s is defined as

$$\varphi_i(s) \triangleq \int_0^\infty \frac{t^i \exp(-t)}{1 + (1-\lambda)(1+s)^i \exp(-st)/\lambda} dt. \quad (37)$$

Proof. See Appendix F. \square

We also observe from (36) that the first term in the right hand side corresponds to the averaged MSE if the user activity is assumed to be known, and the second term corresponds to the extra error brought by unknown user activity.

Based on the expressions of MSE in (34) and (36), the state evolution in (7) can be expressed as

$$\tau_{t+1}^2 = \sigma_w^2 + \frac{N}{L} \text{MSE}(\tau_t), \quad (38)$$

based on which P_F and P_M can be evaluated according to (26), (27), and (31), (32), as functions of the iteration number. As the AMP algorithm converges, τ_t converges to the fixed point τ_∞ of the above equation.

Now we compare the resulting MSEs in these two cases. According to the decomposition of variance, we have

$$\begin{aligned} \mathbb{E}[\text{Var}(X|\tilde{X}^t)] &= \mathbb{E}[\text{Var}(X|\tilde{X}^t, G)] \\ &\quad + \mathbb{E}[\text{Var}(\mathbb{E}[X|\tilde{X}^t, G]|\tilde{X}^t)] \\ &\geq \mathbb{E}[\text{Var}(X|\tilde{X}^t, G)], \end{aligned} \quad (39)$$

which indicates that knowing the large-scale fading can help to improve the estimation on X given \tilde{X}^t . However, the simulation results in Section VI show that surprisingly for the model of the large-scale fading considered in this paper, the performance improvement is actually minor, indicating that knowing the large-scale fading does not help to get a much better estimation. Knowing the exact value of g_n is not crucial in user activity detection and the statistical information of g_n is sufficient for device detection.

V. USER ACTIVITY DETECTION: MULTIPLE-ANTENNA CASE

This section designs the AMP algorithms that account for wireless channel propagation for the massive connectivity problem in the multiple-antenna case. As mentioned earlier, two different AMP algorithms can be used for the MMV problem: the AMP with a vector denoiser operating on each row of the input matrix, or the parallel AMP-MMV that divides the MMV problem into parallel SMV problems and iteratively solves the SMV problem on each antenna separately with soft information exchange between the antennas. The AMP with vector denoiser admits a state evolution, which allows an easier characterization of its performance, whereas AMP-MMV can be implemented in a distributed way which is helpful for reducing the running time of the algorithm, especially when the BS is equipped with large antenna arrays.

A. User Activity Detection by AMP with Vector Denoiser

As in the scenario with single antenna, we consider both the cases where only the statistical knowledge or the exactly knowledge of the large-scale fading is known at the BS. To design the denoisers, we first characterize the pdfs of the row vectors of \mathbf{X} in the following.

Proposition 7. Denote \mathbf{r}_n as the row vector of \mathbf{X} . If only $p_G(g_n)$ is known at the BS, the pdf of \mathbf{r}_n is given by

$$p_{\mathbf{R}}(\mathbf{r}_n) = (1 - \lambda)\delta_{\mathbf{0}} + \int_0^\infty \frac{\exp(-\|\mathbf{r}_n\|_2^2 g_n^{-2})}{\pi^M g_n^{\gamma+2M} / (a\lambda Q(g_n))} dg_n. \quad (40)$$

If g_n is known, the pdf of \mathbf{r}_n is Bernoulli-Gaussian as

$$p_{\mathbf{R}|G}(\mathbf{r}_n|g_n) = (1 - \lambda)\delta_{\mathbf{0}} + \frac{\lambda \exp(-\|\mathbf{r}_n\|_2^2 g_n^{-2})}{(\pi g_n^2)^M}. \quad (41)$$

Proof. The results are extensions of (14) and (18) by considering multivariate random variables. \square

Given $\tilde{\mathbf{R}}^t = \mathbf{R} + \mathbf{U}_n^t$ with \mathbf{U}^t following complex Gaussian distribution with zero mean and covariance Σ_t , the MMSE denoisers $\eta_t(\tilde{\mathbf{r}}_n^t)$ and $\eta_t(\tilde{\mathbf{r}}_n^t, g_n)$ for both cases are given by the conditional expectation in the following.

Proposition 8. If only $p_G(g_n)$ is known at the BS, the conditional expectation of \mathbf{R} given $\tilde{\mathbf{R}}^t = \tilde{\mathbf{r}}_n^t$ is

$$\mathbb{E}[\mathbf{R}|\tilde{\mathbf{R}}^t = \tilde{\mathbf{r}}_n^t] = \frac{\int_0^\infty Q(g_n)\psi_a(g_n)(g_n^{-2}\Sigma_t + \mathbf{I})^{-1}\tilde{\mathbf{r}}_n^t dg_n}{\psi_c(g_n) + \int_0^\infty Q(g_n)\psi_b(g_n)dg_n}, \quad (42)$$

where $\psi_a(g_n)$, $\psi_b(g_n)$ and $\psi_c(g_n)$ are defined as follows

$$\psi_a(g_n) \triangleq \frac{\exp(-\tilde{\mathbf{r}}_n^t (\Sigma_t^{-1} - (\Sigma_t + g_n^{-2}\Sigma_t^2)^{-1}) (\tilde{\mathbf{r}}_n^t)^*)}{g_n^\gamma |\Sigma_t + g_n^2 \mathbf{I}|}, \quad (43)$$

$$\psi_b(g_n) \triangleq \frac{\exp(-\tilde{\mathbf{r}}_n^t (g_n^{-2}\mathbf{I} - (g_n^2\mathbf{I} + g_n^4\Sigma_t^{-1})^{-1}) (\tilde{\mathbf{r}}_n^t)^*)}{g_n^\gamma |\Sigma_t + g_n^2 \mathbf{I}|}, \quad (44)$$

$$\psi_c(g_n) \triangleq (1 - \lambda)(a\lambda)^{-1} \exp(-\tilde{\mathbf{r}}_n^t \Sigma_t^{-1} (\tilde{\mathbf{r}}_n^t)^*) |\Sigma_t|^{-1}. \quad (45)$$

If g_n is known at the BS, the conditional expectation is

$$\mathbb{E}[\mathbf{R}|\tilde{\mathbf{R}}^t = \tilde{\mathbf{r}}_n^t, G = g_n] = \frac{(g_n^{-2}\Sigma_t + \mathbf{I})^{-1}\tilde{\mathbf{r}}_n^t}{1 + \frac{1-\lambda}{\lambda}|g_n^2\mathbf{I} + \Sigma_t| \psi_d(g_n)}, \quad (46)$$

where $\psi_d(g_n)$ is defined as follows

$$\psi_d(g_n) \triangleq \exp(-\tilde{\mathbf{r}}_n^t (\Sigma_t^{-1} - (\Sigma_t + g_n^2\mathbf{I})^{-1}) (\tilde{\mathbf{r}}_n^t)^*) |\Sigma_t|^{-1}. \quad (47)$$

Proof. See Appendix G. \square

The covariance matrix Σ_t in both (42) and (46) is tracked via the state evolution (10), and Σ_t can be further simplified by the following proposition.

Proposition 9. Based on the pdfs in (40) and (41) and the state evolution (10), if the initial covariance matrix Σ_0 is a diagonal matrix with identical diagonal entries, i.e., $\Sigma_0 = \tau_0^2 \mathbf{I}$, then Σ_t stays as a diagonal matrix with identical diagonal entries, i.e., $\Sigma_t = \tau_t^2 \mathbf{I}$, for $t \geq 1$, where τ_t is determined by

$$\tau_{t+1}^2 = \sigma_w^2 + \frac{N}{L} \text{MSE}(\tau_t). \quad (48)$$

If only $p_G(g_n)$ is known at the BS, MSE(τ_t) is given by

$$\begin{aligned} \text{MSE}(\tau_t) &= \int_0^\infty \frac{a\lambda g_n^2 \tau_t^2 Q(g_n)}{g_n^\gamma (g_n^2 + \tau_t^2)} dg_n \\ &\quad + \int_0^\infty \frac{\mu_M(s) - \nu_M^2(s) \xi_M^{-1}(s)}{\Gamma(M+1)(\lambda a s^M)} ds, \end{aligned} \quad (49)$$

where functions $\mu_i(s)$, $\nu_i(s)$ and $\xi_i(s)$ are defined in (35), (16), and (17), respectively, and $\Gamma(\cdot)$ is the Gamma function. If the exact large-scale fading g_n is known at the BS, MSE(τ_t) is given by

$$\begin{aligned} \text{MSE}(\tau_t) &= \int_0^\infty \frac{a\lambda g_n^2 \tau_t^2 Q(g_n)}{g_n^\gamma (g_n^2 + \tau_t^2)} dg_n \\ &\quad + \int_0^\infty \frac{a\lambda Q(g_n) g_n^4}{g_n^\gamma (g_n^2 + \tau_t^2)} \left(1 - \frac{\varphi_M(g_n^2 \tau_t^{-2})}{\Gamma(M+1)}\right) dg_n, \end{aligned} \quad (50)$$

where function $\varphi_i(s)$ is defined in (37).

Proof. See Appendix H. \square

Note that Σ_0 is the noise covariance matrix after the first matched filtering, which is indeed a diagonal matrix with identical diagonal entries. Based on Proposition 9, the MMSE denoiser in (42) can be further simplified as

$$\mathbb{E}[\mathbf{R}|\tilde{\mathbf{r}}_n^t = \tilde{\mathbf{r}}_n^t] = \tilde{\mathbf{r}}_n^t \frac{\nu_M(\|\tilde{\mathbf{r}}_n^t\|_2^2)}{\xi_M(\|\tilde{\mathbf{r}}_n^t\|_2^2)}, \quad (51)$$

where $\nu_i(s)$ and $\xi_i(s)$ are defined in (16) and (17), respectively, and the MMSE denoiser in (46) can be simplified as

$$\begin{aligned} \mathbb{E}[\mathbf{R}|\tilde{\mathbf{R}}^t = \tilde{\mathbf{r}}_n^t, G = g_n] \\ = \frac{g_n^2(g_n^2 + \tau_t^2)^{-1}\tilde{\mathbf{r}}_n^t}{1 + \frac{1-\lambda}{\lambda}(g_n^2 + \tau_t^2)^M \exp(-\Delta\|\tilde{\mathbf{r}}_n^t\|_2^2)}, \end{aligned} \quad (52)$$

where Δ is defined in (20). Note that if we let $M = 1$, (51) and (52) reduce to the denoisers for the single-antenna case in (15) and (19). As mentioned before, we can also pre-compute and store the functions $\nu_M(\cdot)$ and $\xi_M(\cdot)$ in (51) as table lookup.

After the AMP algorithm has converged, we use the likelihood ratio test to perform the user activity detection. Recall that $\tilde{\mathbf{R}}^t = \mathbf{R} + \mathbf{U}^t$ where \mathbf{U}^t follows complex Gaussian distribution. For the case where the large-scale fading is unknown, based on (40) and $p_{\tilde{\mathbf{R}}^t}$ derived in (82) in Appendix G, the likelihood probabilities given that the user is inactive and active are, respectively

$$p_{\tilde{\mathbf{R}}^t|\mathbf{R}}(\tilde{\mathbf{r}}_n^t|\mathbf{R} = \mathbf{0}) = \frac{\exp(-\|\tilde{\mathbf{r}}_n^t\|_2^2\tau_t^{-2})}{\pi^M\tau_t^{2M}}, \quad (53)$$

$$p_{\tilde{\mathbf{R}}^t|\mathbf{R}}(\tilde{\mathbf{r}}_n^t|\mathbf{R} \neq \mathbf{0}) = \int_0^\infty \frac{ag_n^{-\gamma}Q(g_n)}{\pi^M(g_n^2 + \tau_t^2)^M} \exp\left(\frac{-\|\tilde{\mathbf{r}}_n^t\|_2^2}{g_n^2 + \tau_t^2}\right) dg_n. \quad (54)$$

For the case where the large-scale fading coefficient is known, noting that \mathbf{R} follows a Beroulli-Gaussian distribution, and $\tilde{\mathbf{R}}^t$ follows a mixed Gaussian distribution, then the likelihood probabilities can be computed as, respectively

$$p_{\tilde{\mathbf{R}}^t|\mathbf{R},G}(\tilde{\mathbf{r}}_n^t|\mathbf{R} = \mathbf{0}, G = g_n) = \frac{\exp(-\|\tilde{\mathbf{r}}_n^t\|_2^2\tau_t^{-2})}{\pi^M\tau_t^{2M}}, \quad (55)$$

$$p_{\tilde{\mathbf{R}}^t|\mathbf{R},G}(\tilde{\mathbf{r}}_n^t|\mathbf{R} \neq \mathbf{0}, G = g_n) = \frac{\exp(-\|\tilde{\mathbf{r}}_n^t\|_2^2(\tau_t^2 + g_n^2)^{-1})}{\pi^M(\tau_t^2 + g_n^2)^M}. \quad (56)$$

For both cases, we immediately obtain the LLRs as, respectively

$$\text{LLR} = \log \int_0^\infty \frac{a\tau_t^{2M}g_n^{-\gamma}Q(g_n)}{(g_n^2 + \tau_t^2)^M} \exp(\|\tilde{\mathbf{r}}_n^t\|_2^2\Delta) dg_n, \quad (57)$$

$$\text{LLR}(g_n) = \log\left(\frac{\tau_t^{2M}}{(\tau_t^2 + g_n^2)^M} \exp(\|\tilde{\mathbf{r}}_n^t\|_2^2\Delta)\right). \quad (58)$$

Observing that LLRs are monotonic in $\|\tilde{\mathbf{r}}_n^t\|_2$, we can set a threshold l_n on $\|\tilde{\mathbf{r}}_n^t\|_2$ to perform the detection. When the

large-scale fading is unknown at the BS, the probabilities of false alarm or missed detection are then given as, respectively

$$\begin{aligned} P_F &= \int_{\|\tilde{\mathbf{r}}_n^t\|_2 > l_n} \frac{\exp(-\|\tilde{\mathbf{r}}_n^t\|_2^2\tau_t^{-2})}{\pi^M\tau_t^{2M}} d\tilde{\mathbf{r}}_n^t \\ &\stackrel{(a)}{=} 1 - \frac{1}{\Gamma(M)}\bar{\gamma}(M, l_n^2\tau_t^{-2}), \end{aligned} \quad (59)$$

and

$$\begin{aligned} P_M &= \int_{\|\tilde{\mathbf{r}}_n^t\|_2 < l_n} \int_0^\infty \frac{ag_n^{-\gamma}Q(g_n)}{\pi^M(g_n^2 + \tau_t^2)^M} \\ &\quad \exp\left(\frac{-\|\tilde{\mathbf{r}}_n^t\|_2^2}{g_n^2 + \tau_t^2}\right) dg_n d\tilde{\mathbf{r}}_n^t \\ &\stackrel{(b)}{=} \int_0^\infty \frac{ag_n^{-\gamma}Q(g_n)}{\Gamma(M)}\bar{\gamma}(M, l_n^2(g_n^2 + \tau_t^2)^{-1}) dg_n, \end{aligned} \quad (60)$$

where $\bar{\gamma}(\cdot, \cdot)$ is the lower incomplete Gamma function, and (a) and (b) are simply obtained by noticing that the integral of $\tilde{\mathbf{r}}_n^t$ can be interpreted as the cumulative distribution function (cdf) of a χ^2 distribution with $2M$ degrees of freedom since $\|\tilde{\mathbf{r}}_n^t\|_2^2$ can be regarded as a sum of the squares of $2M$ identical real Gaussian random variables. Using the same approach, when the large scale fading is known to the BS, the probabilities of false alarm and missed detection can be evaluated as

$$\begin{aligned} P_F(g_n) &= \int_{\|\tilde{\mathbf{r}}_n^t\|_2 > l_n} \frac{\exp(-\|\tilde{\mathbf{r}}_n^t\|_2^2\tau_t^{-2})}{\pi^M\tau_t^{2M}} d\tilde{\mathbf{r}}_n^t, \\ &= 1 - \frac{1}{\Gamma(M)}\bar{\gamma}(M, l_n^2\tau_t^{-2}), \end{aligned} \quad (61)$$

$$\begin{aligned} P_M(g_n) &= \int_{\|\tilde{\mathbf{r}}_n^t\|_2 < l_n} \frac{\exp(-\|\tilde{\mathbf{r}}_n^t\|_2^2(\tau_t^2 + g_n^2)^{-1})}{\pi^M(\tau_t^2 + g_n^2)^M} d\tilde{\mathbf{r}}_n^t \\ &= \frac{1}{\Gamma(M)}\bar{\gamma}(M, l_n^2(g_n^2 + \tau_t^2)^{-1}). \end{aligned} \quad (62)$$

It is easy to verify that when $M = 1$, (59), (60), (61) and (62) reduce to (26), (27), (31) and (32), respectively.

Based on (59), (60), (61) and (62), we can design the threshold l_n to achieve a trade-off between the probability of false alarm and probability of missed detection. The proposed thresholding strategy in the single-antenna case can still be used in multiple-antenna scenario.

B. User Activity Detection by Parallel AMP-MMV

The outline of the parallel AMP-MMV algorithm is as presented in Algorithm 1. In this section, we adopt the parallel AMP-MMV algorithm for our problem setup; we present the expression of the denoiser, $\eta(\cdot, \mathbf{g}, t, i, m) \triangleq [\eta_{t,i,m}(\cdot, g_1), \dots, \eta_{t,i,m}(\cdot, g_N)]^T$ and the probability of a device being active based on the decision at the m th AMP-SMV stage, $\bar{\pi}_{nm}$. Here we only discuss the case where the large-scale fading is known. The extension to the scenario where the large-scale fading is unknown is similar.

Since the parallel AMP-MMV algorithm employs M parallel AMP-SMVs, the expression of the scalar denoiser for each AMP-SMV is in the form of the MMSE denoiser for the single-antenna case in (19). However, instead of using the prior λ as the probability of being active for each user, the algorithm has access to a better estimate for the probability of activities

as $\hat{\pi}_{nm}$ as algorithm proceeds. Therefore, the expression for the MMSE denoiser can be written as

$$\eta_{t,i,m}(\tilde{x}_{nm}^{t,i}; g_n) = \frac{g_n^2(g_n^2 + \tau_{t,i}^2)^{-1} \tilde{x}_{nm}^{t,i}}{1 + \frac{1 - \hat{\pi}_{nm}}{\hat{\pi}_{nm}} \frac{g_n^2 + \tau_{t,i}^2}{\tau_{t,i}^2} \exp\left(\frac{-g_n^2 |\tilde{x}_{nm}^{t,i}|^2}{\tau_{t,i}^2 (g_n^2 + \tau_{t,i}^2)}\right)}, \quad (63)$$

where $\tilde{x}_{nm}^{t,i}$ and x_{nm} are the elements in the n th row and the m th column of $\tilde{\mathbf{X}}^{t,i}$ and \mathbf{X} , respectively. At the end of the i th outer iteration, i.e., $t = T$, the likelihood probabilities given that the user is inactive or active can be written as

$$p(\tilde{x}_{nm}^{T,i} | X = 0, G = g_n) = \frac{\exp(-|\tilde{x}_{nm}^{T,i}|^2 \tau_{T,i}^{-2})}{\pi \tau_{T,i}^2}, \quad (64)$$

$$p(\tilde{x}_{nm}^{T,i} | X \neq 0, G = g_n) = \frac{\exp(-|\tilde{x}_{nm}^{T,i}|^2 (g_n^2 + \tau_{T,i}^2)^{-1})}{\pi (\tau_{T,i}^2 + g_n^2)}. \quad (65)$$

Further, using equations (64) and (65), the probability that user n is active based on the decision at the m th AMP-SMV can be calculated as

$$\begin{aligned} \hat{\pi}_{nm} &= \frac{p(\tilde{x}_{nm}^{T,i} | X \neq 0, G = g_n)}{p(\tilde{x}_{nm}^{T,i} | X \neq 0, G = g_n) + p(\tilde{x}_{nm}^{T,i} | X = 0, G = g_n)} \\ &= \left(1 + \frac{\tau_{T,i}^2 + g_n^2}{\tau_{T,i}^2} \exp\left(\frac{-g_n^2 |\tilde{x}_{nm}^{T,i}|^2}{\tau_{T,i}^2 (g_n^2 + \tau_{T,i}^2)}\right)\right)^{-1}. \end{aligned} \quad (66)$$

After the parallel AMP-MMV is terminated, we use likelihood ratio test to perform the user activity detection. It can be shown that the LLR for user n can be calculated as

$$\text{LLR}(g_n) = \log \left(\frac{\tau_{T,I}^{2M}}{(\tau_{T,I}^2 + g_n^2)^M} \exp\left(\frac{-g_n^2 \sum_m |\tilde{x}_{nm}^{T,I}|^2}{(\tau_{T,I}^2 + g_n^2) \tau_{T,I}^2}\right) \right). \quad (67)$$

It can be seen that the LLR expression for AMP-MMV algorithm is in a similar form as in (57). Therefore, with the same discussion, we can show that the probabilities of false alarm and missed detection can be further simplified in a form similar to (61) and (62), respectively. To have complete performance prediction analysis, we also need to determine $\tau_{T,I}^2$ in the parallel AMP-MMV algorithm. However, due to the soft information exchange between the antennas, deriving an analytic state evolution for $\tau_{t,i}^2$ is very challenging. The numerical experiments in Section VI show that the performance of parallel AMP-MMV is very similar to AMP with vector denoiser. This observation suggests that the parameter $\tau_{T,I}^2$ for the AMP-MMV algorithm should be similar to the final value of τ_t^2 in AMP with vector denoiser.

We briefly discuss the complexities of AMP with vector denoiser and AMP-MMV. For both algorithms the computational complexities mainly lie in the matched filtering and residual calculation, which depend on the problem size as $O(NLM)$, at each iteration. The advantage of AMP-MMV is that parallel computation is allowed due to the division of MMV problem into several SMV problems.

VI. SIMULATION RESULTS

We evaluate the performance of the proposed method in a cell of radius $R = 1000$ m with potential $N = 4000$ users among which 200 are active, i.e., $\lambda = 0.05$. The channel fading

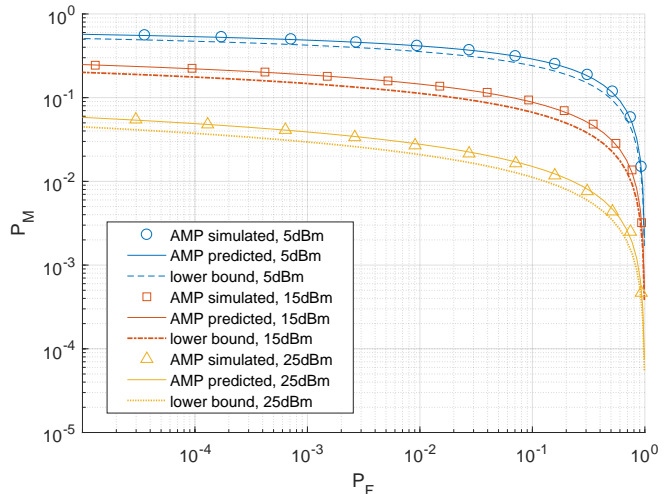


Fig. 2. Performance of AMP based user activity detection with only statistical knowledge of the large-scale fading.

parameters are $\alpha = 15.3$, $\beta = 37.6$ and $\sigma_{\text{SF}} = 8$, and the background noise is -169 dBm/Hz over 10MHz.

We first consider the single-antenna case with only statistical knowledge of large-scale fading. Fig. 2 shows the tradeoff between the probabilities of missed detection and the false alarm of AMP with MMSE denoiser when the pilot sequence length is set as $L = 800$ and the transmit power is set as 5dBm, 15dBm, and 25dBm. We see that the predicted P_M and P_F match the analysis very well. We also plot a lower bound using $\tau_\infty = \sigma_w$. The lower bounds are very close to the actual performance, indicating that after convergence AMP is able to almost completely eliminate multiuser interference; the remaining error is dominated by the background noise.

Fig. 3 shows the performance of the AMP algorithm with MMSE denoiser when the exact large-scale fading coefficients are known. For comparison, the performance with only statistical knowledge of the large-scale fading is also demonstrated (only simulated performance is included since the predicted performance is almost the same as depicted in Fig. 2). Fig. 3 shows that the predicted curves match the simulated curves very well. More interestingly, it indicates that the performance improvement for knowing the exact large-scale fading coefficients is negligible which suggests that knowing the distribution of the large-scale fading (rather than the exact value) is already enough for good user activity detection performance.

The next simulation compares the AMP algorithm with MMSE denoiser with two other algorithms widely used in compressed sensing: CoSaMP [23], and AMP but with soft thresholding denoiser [3]. Compare to AMP, CoSaMP is based on the matching pursuit technique. Compare to AMP with MMSE denoiser, AMP with soft thresholding does not exploit the statistical knowledge of x_n . Fig. 4 shows that AMP with MMSE denoiser outperforms both CoSaMP and AMP with soft thresholding denoiser. This is partly due to the fact that both CoSaMP and AMP with soft thresholding denoiser do

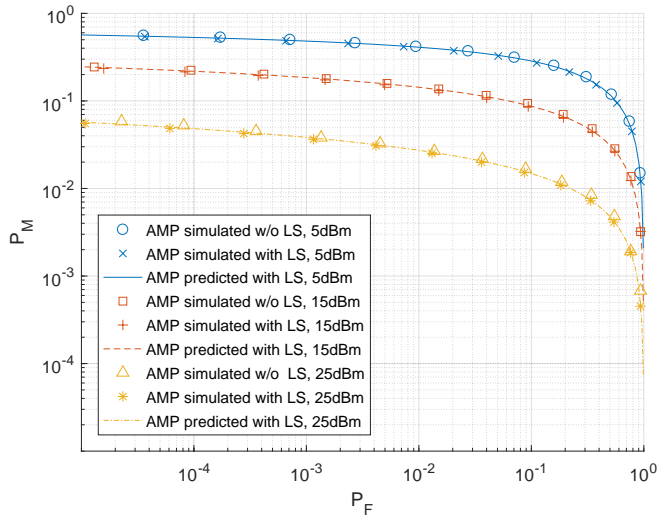


Fig. 3. Performance of AMP based user activity detection with knowledge of the large-scale fading.

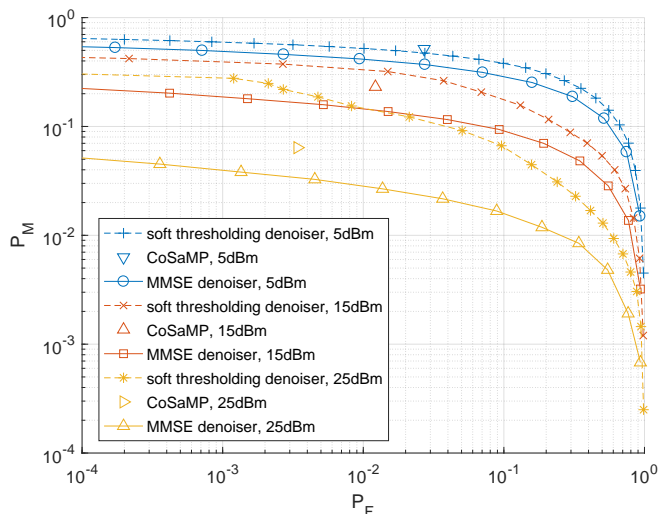


Fig. 4. Performance comparison of AMP with MMSE denoiser, AMP with soft thresholding denoiser, and CoSaMP.

not exploit the the statistical knowledge of x_n . Note that AMP with soft thresholding implicitly solves the LASSO problem [14], [24], i.e., the sparse signal recovery problem as an ℓ_1 -penalized least squares optimization. Therefore, the results in Fig. 4 indicate that AMP with MMSE denoiser also outperforms LASSO.

Fig. 5 compares the performance of the AMP algorithm with MMSE denoiser and the AMP algorithm with soft thresholding denoiser as function of transmit power and pilot length. For convenience, we set $P_F = P_M$ by properly choosing the threshold l . We observe first that the MMSE denoiser outperforms soft thresholding denoiser significantly, but more importantly, we observe that the minimum L needed to drive P_F and P_M to zero as transmit power increases is between 300 and 400 for the MMSE denoiser, whereas the

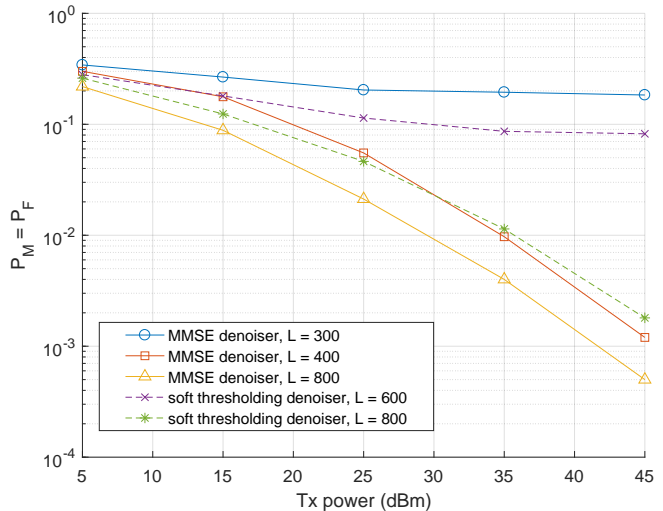


Fig. 5. Impact of transmit power and length of pilot on user activity detection performance: MMSE denoiser vs. soft thresholding denoiser.

minimum L is between 600 and 800 for the soft thresholding denoiser, indicating the clear advantage of accounting for channel statistics in user activity detector design.

Finally, we consider the multiple-antenna case assuming the knowledge of large-scale fading coefficients. Fig. 6 illustrates the probabilities of false alarm and missed detection under different numbers of antennas for both AMP with vector denoiser and parallel AMP-MMV algorithms. For comparison, the single-antenna $M = 1$ case is also included. Fig. 6 shows that for AMP with vector denoiser, the simulated results match the predicted results very well. Further, it shows that the performances of AMP with vector denoiser and parallel AMP-MMV are approximately the same, indicating that although these two algorithms employ different strategies, they both exploit the statistical knowledge of the channel in the same way, resulting in similar performances.

The impact of the pilot length L and the number of antennas M on the probabilities of false alarm and missed detection as the transmit power increases is shown in Fig. 7. We set $L = 300, 600$, and $M = 1, 2, 4$. We make $P_F = P_M$ for convenient comparison by properly choosing the threshold l . Note that in the scenario where the exact large-scale fading coefficients are known, different users have the same probabilities of false alarm but different probabilities of missed detection. Thus we have to use the average probability of missed detection over all users. Fig. 7 shows that increasing L or M brings significant improvement. Specifically, when $L = 300, M = 1$, P_F and P_M tend to remain unchanged as the transmit power increases. However, by either increasing L or increasing M , P_F and P_M can be driven to zero as the transmit power increases. In other words, the minimum L required to drive P_F and P_M to zeros can be reduced by increasing M .

VII. CONCLUSION

This work shows that compressed sensing is a viable strategy for sporadic device activity detection for massive

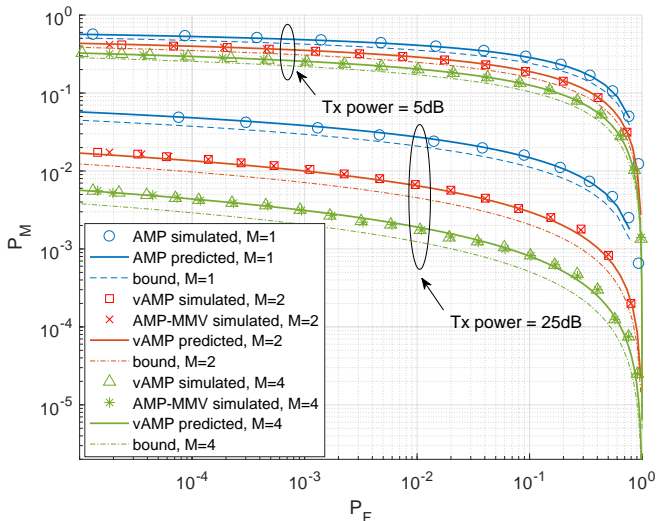


Fig. 6. Performance of AMP with vector denoiser (vAMP) and AMP-MMV for user activity detection in the multiple-antenna case.

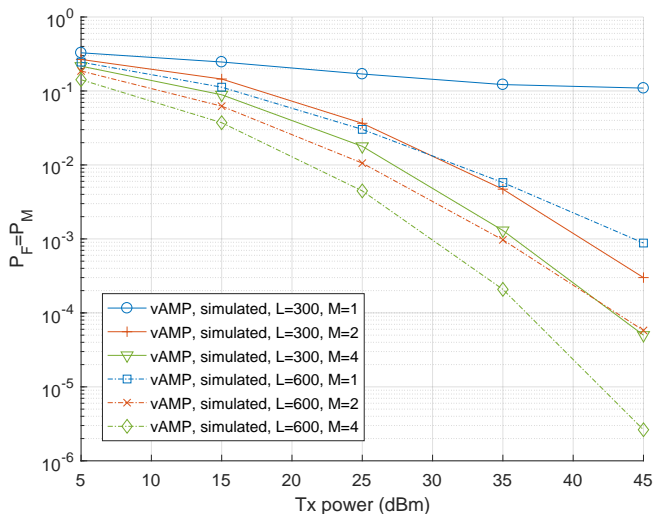


Fig. 7. Impact of length of pilot, number of antennas, and transmit power.

connectivity applications with random non-orthogonal signature sequences. Specifically, we propose an AMP-based user activity detection algorithm by exploiting the statistics of the wireless channel for the uplink of a cellular system with a large number of potential users but only a small fraction of them are active at any time slot. We show that by using the state evolution, a performance characterization in terms of the probabilities of false alarm and missed detection can be accurately predicted. In particular, we consider both cases in which the BS is equipped with a single antenna or multiple antennas. We present the designs of the MMSE denoisers in the scenarios where the large-scale fading is either available exactly or when only its statistics is available at the BS. For the multiple-antenna case, we adopt two AMP algorithms, AMP with vector denoiser and parallel AMP-MMV, to tackle the detection problem. We derive a performance analysis

for both the single-antenna case and the multiple-antenna case. Simulation results validate the analysis, and show that exploiting the statistics of the channel in AMP denoiser design can significantly improve the detection threshold, and further deploying multiple antennas at the BS can also bring significant performance improvement.

APPENDIX

A. Proof of Proposition 1

Denote d, x, y, z as the distance from a user to the BS, the shadowing in dB, the shadowing in linear scale, and the path-loss, respectively. Note that in appendices we slightly abuse some notations appeared in the paper due to the limited alphabet. However this should not cause confusion since they only used for derivations in the appendices. Denote $g \triangleq yz$ as the large-scale fading. We derive the pdfs of d, x, y, z and g as follows.

Assuming that all users are uniformly distributed in the cell with radius R , the pdf of d is

$$p_D(d) = \frac{2d}{R^2}, \quad 0 < d < R. \quad (68)$$

Since $x = -20 \log_{10}(y)$ follows Gaussian distribution with zero mean and variance σ_{SF}^2 , the pdf of y can be derived as

$$p_Y(y) = \frac{20}{\ln(10)\sqrt{2\pi}\sigma_{SF}} \exp\left(-\frac{200 \ln^2(y)}{\ln^2(10)\sigma_{SF}^2}\right). \quad (69)$$

By using $z = 10^{-(\alpha+\beta \log_{10} d)/20}$, we get the pdf of z as

$$p_Z(z) = \frac{40}{R^2\beta} 10^{-2\alpha/\beta} z^{-40/\beta-1}, \quad (70)$$

where $z > 10^{-(\alpha+\beta \log_{10} R)/20}$. The pdf of g is

$$p_G(g) = \int |y|^{-1} p_Y(y) p_Z(y^{-1}g) dy \triangleq a g^{-\gamma} Q(g), \quad (71)$$

where $Q(g) \triangleq \int_{b \ln g + c}^{\infty} \exp(-s^2) ds$, $\gamma \triangleq 40/\beta + 1$, and a, b and c are constants given in the proposition.

B. Proof of Proposition 2

Denote g as the large-scale fading following (11), and $x = x_R + jx_I$ as the Rayleigh fading, where x_R and x_I are the real and imaginary parts of x , respectively. Denote $h = h_R + jh_I$ as the channel coefficient accounting for both large-scale fading g and Rayleigh fading x , i.e., $h = gx$. Then the pdf of h is

$$\begin{aligned} p_H(h) &= \int p_{H_R, H_I, G}(h_R, h_I, g) dg \\ &= \int p_G(g) p_{X_R, X_I}\left(\frac{h_R}{g}, \frac{h_I}{g}\right) \left| \frac{\partial(x_R, x_I, g)}{\partial(h_R, h_I, g)} \right| dg \\ &= \frac{a}{\pi} \int_0^{\infty} g^{-\gamma-2} Q(g) \exp\left(\frac{-|h|^2}{g^2}\right) dg, \end{aligned} \quad (72)$$

where $p_{H_R, H_I, G}(h_R, h_I, g)$ and $p_{X_R, X_I}(x_R, x_I)$ are the joint pdfs, and $\left| \frac{\partial(x_R, x_I, g)}{\partial(h_R, h_I, g)} \right| = g^{-2}$ is the Jacobian determinant. When g is known, $p_{H|G}(h|g)$ follows the complex Gaussian distribution with zero mean and variance g^2 .

C. Proof of Proposition 3

We omit superscript t and subscript n for notation simplicity. The conditional expectation of X given $\tilde{X} = \tilde{x}$ can be expressed as

$$\begin{aligned} \mathbb{E}[X|\tilde{X} = \tilde{x}] &= \int x \frac{p_X(x)}{p_{\tilde{X}}(\tilde{x})} p_{\tilde{X}|X}(\tilde{x}|x) dx \\ &= \iint_0^\infty f(g)x \exp\left(\frac{-|x|^2}{g^2} + \frac{-|\tilde{x} - x|^2}{\tau^2}\right) dg dx \\ &= \iint_0^\infty f(g)x \exp\left(\frac{-|\tilde{x}|^2}{g^2 + \tau^2} + \frac{-|x - \delta\tilde{x}|^2}{\delta\tau^2}\right) dg dx \\ &\stackrel{(a)}{=} \frac{\lambda a \tilde{x}}{p_{\tilde{X}}(\tilde{x})\pi} \int_0^\infty \exp\left(\frac{-|\tilde{x}|^2}{g^2 + \tau^2}\right) \frac{Q(g)g^{2-\gamma}}{(g^2 + \tau^2)^2} dg, \end{aligned} \quad (73)$$

where $f(g) \triangleq \lambda a Q(g)/(p_{\tilde{X}}(\tilde{x})\pi^2\tau^2g^{\gamma+2})$, $\delta \triangleq g^2/(g^2 + \tau^2)$, (a) is obtained by using Gaussian integral of x . By substituting the expression of $p_{\tilde{X}}(\tilde{x})$ derived in Appendix D, we get $\mathbb{E}[X|\tilde{X} = \tilde{x}]$ as in (15).

D. Proof of Proposition 4

We omit superscript t and subscript n in the following. Note that $p_{\tilde{X}|X}(\tilde{x}|X = 0) = p_W(\tilde{x})$ where random variable W is defined as $W \triangleq \tau V$, and $p_{\tilde{X}|X}(\tilde{x}|X \neq 0) = p_Y(\tilde{x})$ where random variable Y is defined as $Y \triangleq H + W$ with H following the distribution in (12). Since V follows complex Gaussian distribution with zero mean and unit variance, we get

$$p_{\tilde{X}|X}(\tilde{x}|X = 0) = \frac{1}{\pi\tau^2} \exp\left(\frac{-|\tilde{x}|^2}{\tau^2}\right), \quad (74)$$

To compute $p_{\tilde{X}|X}(\tilde{x}|X \neq 0)$, we derive $p_Y(y)$ as follows

$$\begin{aligned} p_Y(y) &\stackrel{(a)}{=} \int p_H(y - w)p_W(w) dw \\ &\stackrel{(b)}{=} \int_0^\infty \frac{ag^{-\gamma}Q(g)}{\pi(g^2 + \tau^2)} \exp\left(\frac{-|y|^2}{g^2 + \tau^2}\right) dg, \end{aligned} \quad (75)$$

where (a) is obtained by $p_{Y,W}(y, w) = p_H(y - w)p_W(w)$, and (b) is obtained by substituting (72). Combine the results in (74) and (75) with $p_{\tilde{X}|X}(\tilde{x}|X \neq 0) = p_Y(\tilde{x})$, we get

$$\begin{aligned} p_{\tilde{X}}(\tilde{x}) &= \frac{1 - \lambda}{\pi\tau^2} \exp\left(\frac{-|\tilde{x}|^2}{\tau^2}\right) \\ &\quad + \int_0^\infty \frac{\lambda a Q(g) \exp(-|\tilde{x}|^2/(g^2 + \tau^2))}{\pi g^\gamma (g^2 + \tau^2)} dg. \end{aligned} \quad (76)$$

E. Proof of Proposition 5

We omit superscript t and subscript n for notation simplicity. The conditional variance of X given $\tilde{X} = \tilde{x}$ is

$$\text{Var}(X|\tilde{X} = \tilde{x}) = \mathbb{E}[|X|^2|\tilde{X} = \tilde{x}] - |\mathbb{E}[X|\tilde{X} = \tilde{x}]|^2. \quad (77)$$

Since we have derived $\mathbb{E}[X|\tilde{X} = \tilde{x}]$ in (73), we only need to derive $\mathbb{E}[|X|^2|\tilde{X} = \tilde{x}]$, which can be expressed as

$$\begin{aligned} \mathbb{E}[|X|^2|\tilde{X} = \tilde{x}] &= \int \frac{|x|^2 p_X(x)}{p_{\tilde{X}}(\tilde{x})} p_{\tilde{X}|X}(\tilde{x}|x) dx \\ &= \iint_0^\infty f(g)|x|^2 \exp\left(\frac{-|x|^2}{g^2} + \frac{-|\tilde{x} - x|^2}{\tau^2}\right) dg dx \\ &= \iint_0^\infty f(g)|x|^2 \exp\left(\frac{-|\tilde{x}|^2}{g^2 + \tau^2} + \frac{-|x - \delta\tilde{x}|^2}{\delta\tau^2}\right) dg dx \\ &\stackrel{(a)}{=} \int_0^\infty \frac{\lambda a Q(g) \hat{f}(g)}{g^\gamma p_{\tilde{X}}(\tilde{x})\pi} \exp\left(\frac{-|\tilde{x}|^2}{g^2 + \tau^2}\right) dg, \end{aligned} \quad (78)$$

where $f(g)$ is defined in Appendix C, (a) is obtained by using Gaussian integral of x , $\hat{f}(g) \triangleq \tau^2 g^2/(g^2 + \tau^2)^2 + |\tilde{x}|^2 g^4/(g^2 + \tau^2)^3$. By using (77), (76), (73), and $\text{MSE}(\tau) = \int \text{Var}(X|\tilde{X} = \tilde{x}) p_{\tilde{X}}(\tilde{x}) d\tilde{x}$ with some algebraic manipulations, we obtain (34).

F. Proof of Proposition 6

Similar to Appendix E, we first derive the conditional expectation $\mathbb{E}[|X|^2|\tilde{X} = \tilde{x}, G = g]$ as

$$\mathbb{E}[|X|^2|\tilde{X} = \tilde{x}, G = g] = \frac{\lambda \hat{f}(g) \exp(-|\tilde{x}|^2/(g^2 + \tau^2))}{p_{\tilde{X}|G}(\tilde{x}|g)\pi}, \quad (79)$$

where $\hat{f}(g)$ is defined in Appendix E. Then based on (19) and $\text{Var}(X|\tilde{X} = \tilde{x}, G = g) = \mathbb{E}[|X|^2|\tilde{X} = \tilde{x}, G = g] - |\mathbb{E}[X|\tilde{X} = \tilde{x}, G = g]|^2$, we have

$$\begin{aligned} \text{MSE} &= \iint \text{Var}(X|\tilde{X} = \tilde{x}, G = g) p_{\tilde{X}|G}(\tilde{x}|g) p_G(g) d\tilde{x} dg \\ &\stackrel{(a)}{=} \int_0^\infty \left(\frac{\lambda g^2 \tau^2}{g^2 + \tau^2} + \frac{\lambda g^4 (1 - \varphi_1(g^2 \tau^{-2}))}{g^2 + \tau^2} \right) p_G(g) dg, \end{aligned} \quad (80)$$

where (a) is obtained by using Gaussian integral over \tilde{x} . After plugging $p_G(g)$, we finally get (36).

G. Proof of Proposition 8

We omit superscript t and subscript n . For the case where the large scale fading is unknown, the proof is similar to Appendix C except that we need to deal with random vectors rather than random scalars. By using

$$\mathbb{E}[\mathbf{R}|\tilde{\mathbf{R}} = \tilde{\mathbf{r}}] = \int \mathbf{r} \frac{p_{\mathbf{R}}(\mathbf{r})}{p_{\tilde{\mathbf{R}}}(\tilde{\mathbf{r}})} p_{\tilde{\mathbf{R}}|\mathbf{R}}(\tilde{\mathbf{r}}|\mathbf{r}) d\mathbf{r}, \quad (81)$$

where $p_{\tilde{\mathbf{R}}}(\tilde{\mathbf{r}})$ can be derived as

$$\begin{aligned} p_{\tilde{\mathbf{R}}}(\tilde{\mathbf{r}}) &= \frac{1 - \lambda}{(\pi\tau^2)^M} \exp\left(\frac{-\|\tilde{\mathbf{r}}\|_2^2}{\tau^2}\right) \\ &\quad + \int_0^\infty \frac{\lambda a Q(g) \exp(-\|\tilde{\mathbf{r}}\|_2^2/(g^2 + \tau^2))}{\pi^M g^\gamma (g^2 + \tau^2)^M} dg. \end{aligned} \quad (82)$$

By plugging $p_{\tilde{\mathbf{R}}}(\tilde{\mathbf{r}})$ and $p_{\mathbf{R}}(\mathbf{r})$ into (81), and using multivariate Gaussian integral of \mathbf{r} with some algebraic manipulations, we can obtain (42). For the case where the large-scale fading is known, the conditional expectation can be found in [18].

H. Proof of Proposition 9

Since the proofs for both cases are similar, in the following we focus on the case where the large-scale fading is known. We omit subscript n , and use t as *subscript* instead of superscript for convenience. We use induction by assuming $\Sigma_t = \tau_t^2 \mathbf{I}$ holds. To evaluate the right hand side of (10), we first derive the distribution of $\tilde{\mathbf{R}}_t$ based on (41) as

$$p_{\tilde{\mathbf{R}}_t|G}(\tilde{\mathbf{r}}_t|g) = \frac{\lambda \exp(-\|\tilde{\mathbf{r}}_t\|_2^2 (g^2 + \tau_t^2)^{-1})}{\pi^M (g^2 + \tau_t^2)^M} \phi(\tilde{\mathbf{r}}_t), \quad (83)$$

where $\phi(\tilde{\mathbf{r}}_t) \triangleq 1 + (1 - \lambda)(1 + g^2 \tau_t^{-2})^M \exp(-\Delta \|\tilde{\mathbf{r}}_t\|_2^2) / \lambda$, and Δ is defined in (20). We then compute the conditional covariance matrix of \mathbf{R}_t given $\tilde{\mathbf{R}}_t = \tilde{\mathbf{r}}_t$ and $G = g$ as

$$\begin{aligned} \text{Cov} &= \mathbb{E}[\mathbf{R}_t^T (\mathbf{R}_t^T)^* | \tilde{\mathbf{R}}_t = \tilde{\mathbf{r}}_t, G = g] \\ &\quad - \mathbb{E}[\mathbf{R}_t^T | \tilde{\mathbf{R}}_t = \tilde{\mathbf{r}}_t, G = g] (\mathbb{E}[\mathbf{R}_t^T | \tilde{\mathbf{R}}_t = \tilde{\mathbf{r}}_t, G = g])^* \\ &= \frac{g^2 \tau_t^2 \phi^{-1}(\tilde{\mathbf{r}}_t)}{g^2 + \tau_t^2} \mathbf{I} + \frac{\phi^{-1}(\tilde{\mathbf{r}}_t) - \phi^{-2}(\tilde{\mathbf{r}}_t)}{g^{-4}(g^2 + \tau_t^2)^2} \tilde{\mathbf{r}}_t^T (\tilde{\mathbf{r}}_t^T)^*. \end{aligned} \quad (84)$$

Then by taking the expectation over $\tilde{\mathbf{R}}_t$, we obtain

$$\mathbb{E}_{\tilde{\mathbf{R}}_t|G}[\text{Cov}] = \int p_{\tilde{\mathbf{R}}_t|G}(\tilde{\mathbf{r}}_t|g) \text{Cov} d\tilde{\mathbf{r}}_t, \quad (85)$$

which is a diagonal matrix due to fact that the off-diagonal element is an integral of an odd function over a symmetric interval, which is zero. Furthermore, it is easy to observe from the integral that the diagonal elements of $\mathbb{E}_{\tilde{\mathbf{R}}_t|G}[\text{Cov}]$ are identical. Note that when MMSE denoiser is employed, the right hand side of (10) can be rewritten as $\mathbb{E}[\mathbf{D}_t \mathbf{D}_t^*] = \mathbb{E}_G[\mathbb{E}_{\tilde{\mathbf{R}}_t|G}[\text{Cov}]]$, which leads to the result that $\mathbb{E}[\mathbf{D}_t \mathbf{D}_t^*]$ is also a diagonal matrix with identical diagonal elements.

In the following, we derive an explicit expression of $\mathbb{E}[\mathbf{D}_t \mathbf{D}_t^*]$. To this end, we first compute $\mathbb{E}_{\tilde{\mathbf{R}}_t|G}[\text{Cov}]$. Denote c_i as the i th diagonal entry of $\mathbb{E}_{\tilde{\mathbf{R}}_t|G}[\text{Cov}]$, and $\tilde{r}_{t,i}$ is the i th entry of $\tilde{\mathbf{r}}_t$. Based on (84) and (85), we have

$$\begin{aligned} c_i &= \int \frac{g^2 \tau_t^2}{g^2 + \tau_t^2} \cdot \frac{\lambda \exp(-\|\tilde{\mathbf{r}}_t\|_2^2 / (g^2 + \tau_t^2))}{\pi^M (g^2 + \tau_t^2)^M} d\tilde{\mathbf{r}}_t \\ &\quad + \int \frac{|\tilde{r}_{t,i}|^2 (1 - \phi^{-1}(\tilde{\mathbf{r}}_t))}{g^{-4}(g^2 + \tau_t^2)^2} \cdot \frac{\lambda \exp(-\|\tilde{\mathbf{r}}_t\|_2^2 / (g^2 + \tau_t^2))}{\pi^M (g^2 + \tau_t^2)^M} d\tilde{\mathbf{r}}_t \\ &= \frac{\lambda g^2 \tau_t^2}{g^2 + \tau_t^2} + \frac{\lambda g^4}{g^2 + \tau_t^2} \left(1 - \frac{\varphi_M(g^2 \tau_t^{-2})}{\Gamma(M+1)} \right), \end{aligned} \quad (86)$$

where the first term of the last step is obtained by using Gaussian integral, the second term is obtained by integrating in spherical coordinates instead of Cartesian coordinates, and function $\varphi_i(s)$ is defined in (37). As expected, c_i does not depend on i , indicating that the diagonal elements are indeed identical. By replacing g by G and c_i by C , we get $\mathbb{E}[\mathbf{D}_t \mathbf{D}_t^*] = \mathbb{E}_G[C] \mathbf{I}$, where C is a random variable depends on G , and

$$\begin{aligned} \mathbb{E}_G[C] &= \int_0^\infty \frac{aQ(g)}{g^\gamma} \cdot \frac{\lambda g^2 \tau_t^2}{g^2 + \tau_t^2} dg \\ &\quad + \int_0^\infty \frac{aQ(g)}{g^\gamma} \cdot \frac{\lambda g^4}{g^2 + \tau_t^2} \left(1 - \frac{\varphi_M(g^2 \tau_t^{-2})}{\Gamma(M+1)} \right) dg. \end{aligned} \quad (87)$$

The state evolution in (10) is then simplified to

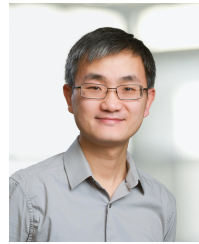
$$\Sigma_{t+1} = \sigma_w^2 \mathbf{I} + \frac{N}{L} \mathbb{E}_G[C] \mathbf{I} \triangleq \tau_{t+1}^2 \mathbf{I}, \quad (88)$$

which completes the induction.

REFERENCES

- [1] J. G. Andrews, S. Buzzi, W. Choi, S. V. Hanly, A. Lozano, A. C. Soong, and J. C. Zhang, "What will 5G be?" *IEEE J. Sel. Areas Commun.*, vol. 32, no. 6, pp. 1065–1082, June 2014.
- [2] W. Yu, "On the fundamental limits of massive connectivity," in *Information Theory and Application (ITA) Workshop*, San Diego, CA, USA, Feb. 2017.
- [3] D. Donoho, A. Maleki, and A. Montanari, "Message-passing algorithms for compressed sensing," *Proc. Nat. Acad. Sci.*, vol. 106, no. 45, pp. 18 914–18 919, Nov. 2009.
- [4] X. Chen, T.-Y. Chen, and D. Guo, "Capacity of Gaussian many-access channels," *IEEE Trans. Inf. Theory*, vol. 63, no. 6, pp. 3516–3539, June 2017.
- [5] H. F. Schepker, C. Bockelmann, and A. Dekorsy, "Exploiting sparsity in channel and data estimation for sporadic multi-user communication," in *Inter. Symp. Wireless Commun. Sys. (ISWCS)*, Ilmenau, Germany, Aug. 2013, pp. 1–5.
- [6] X. Xu, X. Rao, and V. K. N. Lau, "Active user detection and channel estimation in uplink CRAN systems," in *IEEE Inter. Conf. Commun. (ICC)*, London, UK, June 2015, pp. 2727–2732.
- [7] G. Wunder, P. Jung, and M. Ramadan, "Compressive random access using a common overloaded control channel," in *IEEE Globecom Workshops*, San Diego, CA, USA, Dec. 2015, pp. 1–6.
- [8] G. Wunder, H. Boche, T. Strohmer, and P. Jung, "Sparse signal processing concepts for efficient 5G system design," *IEEE Access*, vol. 3, pp. 195–208, Feb. 2015.
- [9] H. Zhu and G. B. Giannakis, "Exploiting sparse user activity in multiuser detection," *IEEE Trans. Commun.*, vol. 59, no. 2, pp. 454–465, Feb. 2011.
- [10] H. F. Schepker and A. Dekorsy, "Compressive sensing multi-user detection with block-wise orthogonal least squares," in *IEEE Veh. Technol. Conf. (VTC Spring)*, Yokohama, Japan, May 2012, pp. 1–5.
- [11] J. Luo and D. Guo, "Neighbor discovery in wireless ad hoc networks based on group testing," in *Allerton Conf. on Commun., Control, and Computing*, Urbana-Champaign, IL, USA, Sep. 2008, pp. 791–797.
- [12] L. Zhang, J. Luo, and D. Guo, "Neighbor discovery for wireless networks via compressed sensing," *Performance Evaluation*, vol. 70, no. 7, pp. 457–471, July 2013.
- [13] M. Bayati and A. Montanari, "The dynamics of message passing on dense graphs, with applications to compressed sensing," *IEEE Trans. Inf. Theory*, vol. 57, no. 2, pp. 764–785, Feb. 2011.
- [14] A. Maleki, L. Anitori, Z. Yang, and R. G. Baraniuk, "Asymptotic analysis of complex LASSO via complex approximate message passing (CAMP)," *IEEE Trans. Inf. Theory*, vol. 59, no. 7, pp. 4290–4308, July 2013.
- [15] S. Rangan, "Generalized approximate message passing for estimation with random linear mixing," in *IEEE Inter. Symp. Inf. Theory (ISIT)*, St. Petersburg, Russia, July 2011, pp. 2168–2172.
- [16] D. L. Donoho, A. Maleki, and A. Montanari, "Message passing algorithms for compressed sensing: I. motivation and construction," in *IEEE Inf. Theory Workshop (ITW)*, Cairo, Egypt, Jan. 2010, pp. 1–5.
- [17] P. Schniter, "Turbo reconstruction of structured sparse signals," in *Annual Conf. on Information Sciences and Systems (CISS)*, Princeton, NJ, USA, Mar. 2010, pp. 1–6.
- [18] J. Kim, W. Chang, B. Jung, D. Baron, and J. C. Ye, "Belief propagation for joint sparse recovery," [Online] available: <http://arxiv.org/abs/1102.3289v1>, 2011.
- [19] J. Ziniel and P. Schniter, "Efficient high-dimensional inference in the multiple measurement vector problem," *IEEE Trans. Signal Process.*, vol. 61, no. 2, pp. 340–354, Jan. 2013.
- [20] G. Hannak, M. Mayer, A. Jung, G. Matz, and N. Goertz, "Joint channel estimation and activity detection for multiuser communication systems," in *IEEE Inter. Conf. Commun. (ICC) Workshop*, London, UK, June 2015, pp. 2086–2091.
- [21] D. L. Donoho, I. Johnstone, and A. Montanari, "Accurate prediction of phase transitions in compressed sensing via a connection to minimax denoising," *IEEE Trans. Inf. Theory*, vol. 59, no. 6, pp. 3396–3433, June 2013.

- [22] A. Montanari, "Graphical models concepts in compressed sensing," in *Compressed Sensing: Theory and Applications*, Y. C. Eldar and G. Kutyniok, Eds. New York: Cambridge University Press, 2012, ch. 9, pp. 394–438.
- [23] D. Needell and J. A. Tropp, "CoSaMP: Iterative signal recovery from incomplete and inaccurate samples," *Appl. Comp. Harmonic Anal.*, vol. 26, no. 3, pp. 301–321, May 2009.
- [24] D. L. Donoho, A. Maleki, and A. Montanari, "The noise-sensitivity phase transition in compressed sensing," *IEEE Trans. Inf. Theory*, vol. 57, no. 10, pp. 6920–6941, Oct. 2011.



Wei Yu (S'97-M'02-SM'08-F'14) received the B.A.Sc. degree in Computer Engineering and Mathematics from the University of Waterloo, Waterloo, Ontario, Canada in 1997 and M.S. and Ph.D. degrees in Electrical Engineering from Stanford University, Stanford, CA, in 1998 and 2002, respectively. Since 2002, he has been with the Electrical and Computer Engineering Department at the University of Toronto, Toronto, Ontario, Canada, where he is now Professor and holds a Canada Research Chair (Tier 1) in Information Theory and Wireless Communications. His main research interests include information theory, optimization, wireless communications and broadband access networks.

Prof. Wei Yu currently serves on the IEEE Information Theory Society Board of Governors (2015-20). He serves as the Chair of the Signal Processing for Communications and Networking Technical Committee of the IEEE Signal Processing Society (2017-18). He was an IEEE Communications Society Distinguished Lecturer (2015-16). He currently serves as an Area Editor of the IEEE TRANSACTIONS ON WIRELESS COMMUNICATIONS (2017-19). He served as an Associate Editor for IEEE TRANSACTIONS ON INFORMATION THEORY (2010-2013), as an Editor for IEEE TRANSACTIONS ON COMMUNICATIONS (2009-2011), as an Editor for IEEE TRANSACTIONS ON WIRELESS COMMUNICATIONS (2004-2007), and as a Guest Editor for a number of special issues for the IEEE JOURNAL ON SELECTED AREAS IN COMMUNICATIONS and the EURASIP JOURNAL ON APPLIED SIGNAL PROCESSING. He was a Technical Program co-chair of the IEEE Communication Theory Workshop in 2014, and a Technical Program Committee co-chair of the Communication Theory Symposium at the IEEE International Conference on Communications (ICC) in 2012. Prof. Wei Yu received the IEEE Signal Processing Society Best Paper Award in 2017 and in 2008, a JOURNAL OF COMMUNICATIONS AND NETWORKS Best Paper Award in 2017, a Steacie Memorial Fellowship in 2015, an IEEE Communications Society Best Tutorial Paper Award in 2015, an IEEE ICC Best Paper Award in 2013, the McCharles Prize for Early Career Research Distinction in 2008, the Early Career Teaching Award from the Faculty of Applied Science and Engineering, University of Toronto in 2007, and an Early Researcher Award from Ontario in 2006. Prof. Wei Yu is recognized as a Highly Cited Researcher. He is a Fellow of the Canadian Academy of Engineering.



Zhilin Chen (S'14) received the B.E. degree in electrical and information engineering and the M.E. degree in signal and information processing from Beihang University (BUAA), Beijing, China, in 2012 and 2015, respectively. He is currently pursuing the Ph.D. degree at the University of Toronto, Toronto, ON, Canada. His main research interests include wireless communication and signal processing.



Foad Sohrabi (S'13) received his B.A.Sc. degree in 2011 from the University of Tehran, Tehran, Iran, and his M.A.Sc. degree in 2013 from McMaster University, Hamilton, ON, Canada, both in Electrical and Computer Engineering. Since September 2013, he has been a Ph.D student at University of Toronto, Toronto, ON, Canada. From July to December 2015, he was a research intern at Bell-Labs, Alcatel-Lucent, in Stuttgart, Germany. His main research interests include MIMO communications, optimization theory, wireless communications, and signal processing. He received an IEEE Signal Processing Society Best Paper Award in 2017.